Research Square

Preprints are preliminary reports that have not undergone peer review.
They should not be considered conclusive, used to inform clinical practice,
or referenced by the media as validated information.

# Prediction of Ephemeral Plant Diversity Patterns and Identification of Conservation Priority Areas in the Gurbantünggüt Desert

**Xu Sun**
Shihezi University
**Xiaoxue Zhang**
Shihezi University
**Yang Xue**
Shihezi University
**Songmei Ma**
songmei0618@stu.shzu.edu.cn

Shihezi University
**Xintong Hu**
Shihezi University
**He Sun**
Shihezi University
**Jingjing Zhao**
Shihezi University

**Research Article**

**Keywords:** Ephemeral plants, Species distribution ensemble models, Environmental drivers, Climate velocity, Priority conservation areas

**Posted Date:** May 20th, 2026

**DOI:** https://doi.org/10.21203/rs.3.rs-9428959/v1

**License:** This work is licensed under a Creative Commons Attribution 4.0 International License.
Read Full License

**Additional Declarations:** No competing interests reported.

# Prediction of Ephemeral Plant Diversity Patterns and Identification of Conservation Priority Areas in the Gurbantünggüt Desert

Xu Sun[a],Xiaoxue Zhang[a],Yang Xue[a],Songmei Ma[a,*],Xintong Hu[a],He Sun[a],Jingjing Zhao[a]

[a] *College of Urban and Environmental Sciences, Shihezi University, Shihezi 832003, China*

** Corresponding author. E-mail address: songmei0618@stu.shzu.edu.cn (S.M. Ma),*

*Corresponding author address: No. 221, Shihezi City, XinJiang North Fourth Road, China*

*Contribution: The first two authors contributed equally to this work.*

## Abstract

**Background** Ephemeral plants are a key functional group in the Gurbantunggut Desert, contributing to windbreak, sand fixation, and biodiversity maintenance, while being highly sensitive to climate change. Understanding their spatial diversity patterns can reveal desert ecosystem adaptation mechanisms and inform conservation planning. This study examined 35 dominant ephemeral plant species in the Gurbantunggut Desert, Xinjiang. Using species occurrence data and 12 environmental variables, an ensemble species distribution model was applied to simulate spatial patterns of species richness and migration under current and future (2050s) climate scenarios (SSP1-2.6, SSP2-4.5, SSP3-7.0, SSP5-8.5). Climate velocity was calculated using the KNN algorithm. The Zonation model, integrating species richness, species loss, and climate velocity, was used to identify and optimize priority conservation areas.

**Results** This study show that: (1) species richness declines under all scenarios toward the 2050s, with greater losses under higher emission pathways; the central southern margin consistently remains a biodiversity hotspot. (2) Climate velocity of temperature variables is higher in eastern and western regions, while precipitation variables show higher values in the east; overall, precipitation velocity exceeds temperature velocity. (3) Current conservation areas ($2.103 \times 10^4$ km$^2$) are mainly in southern, western, and eastern regions. By the 2050s, conservation areas shrink ($\approx 1.48–1.58 \times 10^4$ km$^2$) and shift, with higher-priority areas increasingly concentrated in the central southern margin and western desert under higher emission scenarios.

**Conclusion** Future climate change will reduce ephemeral plant diversity and shift priority conservation areas, highlighting the need to protect the central southern margin and western desert.

**Key words:** Ephemeral plants; Species distribution ensemble models; Environmental drivers; Climate velocity; Priority conservation areas.

## 1. Introduction

Climate change is reshaping global species distribution patterns and has become one of the primary drivers of biodiversity loss in the 21st century (Watson et al., 2012). Projections indicate that under a moderate warming scenario by 2050, approximately 15%–37% of global species will face extinction risks across regions covering about 20% of the Earth's terrestrial surface (Thomas et al., 2004). As one of the regions most sensitive to climate change and with the most fragile ecological carrying

capacity (Sheng, 2024), desert ecosystems are confronted with particularly severe challenges: their warming rates significantly exceed the global average, while simultaneously experiencing multiple stressors, including restructured precipitation regimes and increasing alternation of extreme drought and heavy rainfall events (Huang et al., 2016). Such drastic environmental changes intensify habitat fragmentation, reduce suitable distribution areas, and compress ecological niche space (Chen et al., 2011), profoundly reshaping species survival patterns in desert regions and posing multi-level, cumulative threats to ecological security in arid zones (IPCC, 2022).In this context, strengthening biodiversity conservation has become a critical strategy for enhancing regional climate resilience and supporting sustainable development. Area-based conservation strategies, represented by protected areas, serve as key approaches to mitigating habitat degradation and maintaining species persistence. Accurately identifying priority conservation areas (Bellard et al., 2012) aims to accommodate shifts in species distributions, thereby improving the adaptive capacity and long-term resilience of biodiversity conservation under global change. Species distribution models (SDMs) are core tools for predicting species distribution patterns under climate change, and ensemble modeling that integrates multiple algorithms can significantly improve prediction robustness and accuracy (Zhao et al., 2021; Fang et al., 2020; Huang et al., 2023). Currently, simulating species richness patterns under future climate scenarios and identifying areas of high richness as priority conservation zones using conservation planning tools has become a mainstream approach in biodiversity spatial planning (Kanagaraj et al., 2019; Guisan

et al., 2013).The Zonation model, as an advanced tool for identifying priority conservation areas, can comprehensively incorporate multiple conservation cost factors and generate a continuous spatial prioritization of species conservation by iteratively removing spatial units with the lowest conservation value (Zhu et al., 2024). In recent years, incorporating climate velocity (i.e., the theoretical migration rate required for species to track suitable climatic conditions) as a cost layer into the Zonation model has become a research hotspot in species conservation studies (Lai et al., 2022). However, existing planning approaches primarily focus on protecting biodiversity hotspots and have not systematically integrated species loss risks under regional climate change, resulting in insufficient comprehensiveness of conservation strategies. To address this limitation, this study innovatively integrates biodiversity hotspots with high-risk areas of species loss to construct a comprehensive conservation framework, thereby enhancing the precision and rationality of biodiversity conservation.This study focuses on desert plant taxa and identifies priority conservation areas under different climate scenarios by coupling multi-model ensemble approaches with multi-scenario analyses. It aims to develop a dynamic and forward-looking spatial conservation framework to support subsequent design of species migration corridors and optimization of adaptive conservation networks. Ephemeral plants are a group of herbaceous species adapted to the unique climatic conditions of arid regions, completing their life cycle rapidly—within approximately two months—by utilizing early spring precipitation, snowmelt, and rising temperatures (Mao, 1992; Mao & Zhang, 1994). In China, these plants are distributed

exclusively in the northern foothills of the Tianshan Mountains and the Junggar Basin in northern Xinjiang (Mao & Zhang, 1994; Li et al., 1998; Zhang, 2002), comprising more than 200 species across 27 families and 94 genera, accounting for approximately 25% of the total plant families in the Xinjiang flora (Yuan & Tang, 2010).In the Gurbantunggut Desert, the snow cover period in winter lasts for 70–130 days, and early spring snowmelt combined with concentrated winter–spring precipitation (accounting for approximately 44.3% of annual precipitation) provides critical hydrothermal conditions for the germination and rapid growth of ephemeral plants (Mao & Zhang, 1994; Zhang & Chen, 2002; Chen et al., 2019). This unique phenological window makes ephemeral plants a crucial component of plant diversity in this desert: during May, when aeolian activity is intense, vegetation cover can exceed 40%, forming a distinctive feature that differentiates it from other deserts in China.

Ephemeral plants exhibit representative species composition, encompassing taxa such as Brassicaceae, Asteraceae, Boraginaceae, Liliaceae, Poaceae, Fabaceae, and Apiaceae (Qian et al., 2007), and play multiple critical roles in ecosystem structure and function. Following disturbance of sandy surfaces, they act as pioneer colonizers, accounting for more than 80% of the total individuals of invading plants (Wang et al., 2006). During the windy season (April–June), they maintain relatively high vegetation cover, effectively enhancing surface stability (Wang et al., 2004). In the herbaceous layer of communities dominated by species such as Haloxylon ammodendron, ephemeral plants occupy the primary proportion of coverage (often exceeding 50%,

and locally reaching 80–90%), thereby promoting vegetation succession (Zhang & Chen, 2002). Therefore, ephemeral plants are not only important ecological components of fixed and semi-fixed sandy lands in the Gurbantunggut Desert, but also key targets for regional biodiversity conservation and ecosystem management.

At present, studies on early-spring ephemeral plants in Xinjiang have covered aspects such as biological characteristics, functional traits, stoichiometric features, staggered germination, and biomass allocation. However, existing research has largely focused on specific species or localized sampling sites, and has not yet systematically elucidated the overall spatial patterns of ephemeral plant diversity in the Gurbantunggut Desert or their response mechanisms to climate change. In the context of global climate change, several key scientific questions urgently need to be addressed: (1) how will the spatial distribution patterns of ephemeral plant species diversity evolve under current and future climate scenarios? (2) what are the key environmental factors constraining their distribution? and (3) how can climate-adaptive conservation networks for ephemeral plant diversity be constructed based on these insights? Addressing these questions is of great significance for revealing the mechanisms underlying biodiversity maintenance in arid regions and for promoting adaptive conservation of desert ecosystems in Xinjiang.Accordingly, this study focuses on 35 typical ephemeral plant species in the Gurbantunggut Desert. By integrating species occurrence data with 12 environmental variables, we employed the Biomod2 platform to ensemble 11 ecological niche models to simulate the spatial patterns of species richness under current conditions and four future climate scenarios

(2050s; SSP1-2.6, SSP2-4.5, SSP3-7.0, and SSP5-8.5). Furthermore, by incorporating climate velocity estimated using a nearest-neighbor search algorithm and applying the Zonation model, we identified hierarchical priority conservation areas for ephemeral plants under climate change. The results are expected to provide a scientific basis for precise conservation of ephemeral plants and adaptive management of desert ecosystems in arid regions, and to offer new pathways for research on plant diversity responses and conservation planning under climate change.

## 2. Materials and methods

### 2.1 The study area

The Gurbantunggut Desert (44°07′25″–46°23′55″N, 85°10′31″–90°54′11″E), located in the hinterland of the Junggar Basin in Xinjiang, is the largest fixed and semi-fixed desert in China. The region is characterized by a typical temperate continental arid climate, with a mean annual precipitation of 70–150 mm, primarily concentrated in spring and summer, and a mean annual temperature ranging from 6 to 10 °C. The climate exhibits cold winters, hot summers, and pronounced diurnal temperature variations. The geomorphology is dominated by sand ridges, dunes, and inter-dune flatlands. The soils mainly consist of aeolian sandy soils and desert gray calcareous soils, which are generally alkaline and low in organic matter content (Liu, 2020). Surface runoff is extremely scarce, and vegetation growth primarily depends on spring snowmelt and sporadic precipitation (Figure. 1).

Under the influence of a distinctive hydrothermal regime, this desert has

developed a unique vegetation pattern dominated by ephemeral plants and drought-tolerant shrubs. Ephemeral plants rapidly complete their life cycle following snowmelt in spring, forming a pronounced seasonal ground cover and serving as a key functional group within the ecosystem. As one of the centers of ephemeral plant diversity in the arid regions of Central Asia, the flora in this area is primarily composed of species from the Brassicaceae, Boraginaceae, Poaceae, and Asteraceae families, which play irreplaceable ecological roles in maintaining surface stability, preventing wind erosion and sand movement, and facilitating material cycling.

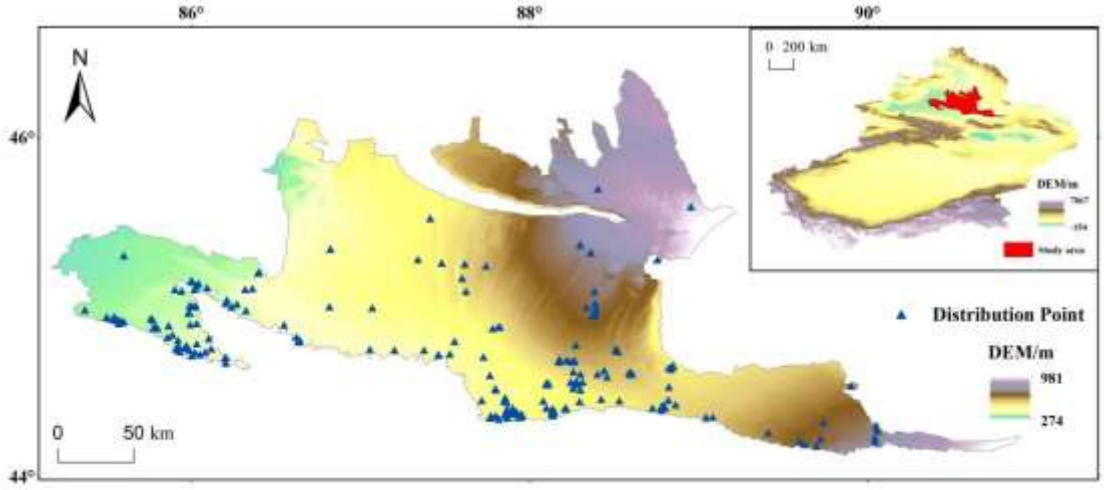



**Figure 1.** Study area and ephemeral plant distribution in Gurbantunggut Desert.

## 2.2 Sources of data and processing

By consulting the Flora of China (online edition), the Flora of Xinjiang, and related literature, a checklist of ephemeral plant species in the Gurbantünggüt Desert was established in this study. Species occurrence records were compiled from multiple sources, including the Chinese Virtual Herbarium (CVH), Plant Plus of China, the National Specimen Information Infrastructure (NSII), the Global

Biodiversity Information Facility, teaching specimen resource-sharing platforms, local floras of Xinjiang, and field surveys. Geographic coordinates for each occurrence record were obtained and corrected using BIGMAP Map Downloader and the China Gazetteer.To reduce spatial autocorrelation, only one occurrence point was retained within each 1 km × 1 km grid cell across the study area using the SDMtools package (Brown, 2014). Ultimately, species with no fewer than five occurrence records were selected for modeling, resulting in a total of 35 species and 373 occurrence records.

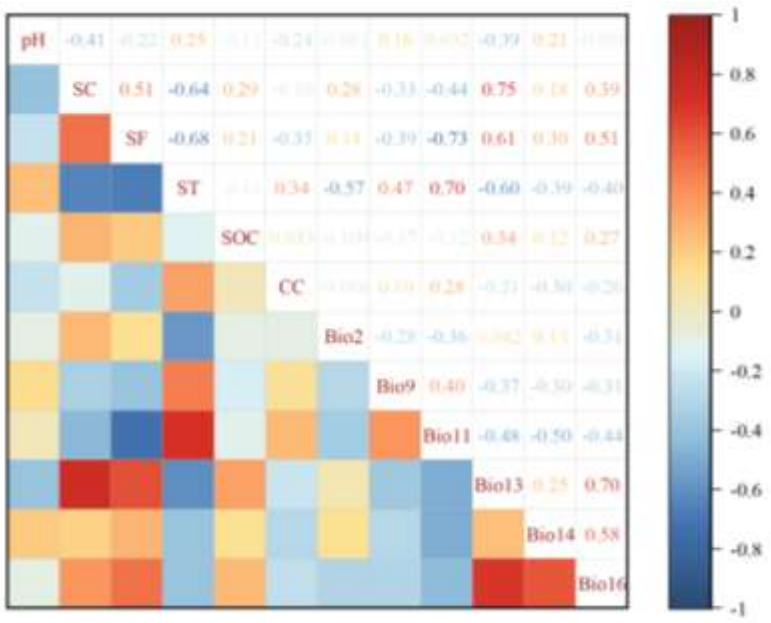
Environmental variables for the current period were obtained from the WorldClim 2.1 dataset (1970–2000), including 19 bioclimatic variables, elevation, as well as soil and snow data, totaling 28 environmental variables (see Table 1 for details). For the future period (2050s, 2040–2060), climate data were derived from the BCC-CSM2-MR model provided by WorldClim 2.1, encompassing 19 bioclimatic variables under four Shared Socioeconomic Pathways (SSPs): SSP1-2.6, SSP2-4.5, SSP3-7.0, and SSP5-8.5. All data have a spatial resolution of 30 arc-seconds.

**Table 1.** Information and Sources of Environmental Variables

| Variable | Spatial Resolution | Data Source |
|---|---|---|
| Temperature variables(Bio1—Bio11) | 30s | Worldclim 2.1 |
| Precipitation variables(Bio12—Bio19) | 30s | Worldclim 2.1 |
| Elevation（ELE） | 30s | Worldclim 2.1 |

| | | |
|---|---|---|
| Soil pH（pH) | 250m | SoilGrid |
| Soil sand content（SAC） | 250m | SoilGrid |
| Soil silt content（SC） | 250m | SoilGrid |
| Soil clay content（CC） | 250m | SoilGrid |
| Soil organic carbon（SOC） | 250m | SoilGrid |
| Snow end date(SF) | 500m | National Cryosphere Desert Science Data Center |
| Snow start date(ST) | 500m | National Cryosphere Desert Science Data Center |
| Snow duration(SE) | 500m | National Cryosphere Desert Science Data Center |

To ensure the consistency of subsequent model simulations, all environmental variables in this study were resampled to a uniform spatial resolution of 30 arc-seconds while maintaining a consistent geographic extent. Furthermore, considering that highly correlated factors may lead to model overfitting, variance inflation factor (VIF) and Pearson correlation analyses were conducted on the selected environmental variables using the "usdm" package in R 4.4.1. Environmental variables with Pearson correlation coefficients below 0.8 and VIF values below 10 were retained for subsequent species distribution model construction (Fan et al., 2024), resulting in a final set of 12 environmental factors (Figure. 2).




192

193 **Figure 2.** Pearson Correlation Matrix of Environmental Variables Used in Species Distribution

194 Modeling

195 **2.3. Simulation of Annual Plant Species Richness Patterns**

196 Based on distribution point data of 35 annual plant species and the selected

197 environmental variables, this study employed the Biomod2 platform to integrate 11

198 ecological niche models to simulate the suitable habitat distribution for each species.

199 The models used included: Generalized Linear Model (GLM), Generalized Boosted

200 Model (GBM), Generalized Additive Model (GAM), Classification and Regression

201 Tree (CTA), Artificial Neural Network (ANN), Flexible Discriminant Analysis (FDA),

202 Surface Range Envelope (SRE), Multivariate Adaptive Regression Splines (MARS),

203 Random Forest (RF), Maximum Entropy Network (MAXNET), and Extreme

204 Gradient Boosting (XGBOOST). During modeling, 1,000 pseudo-absence points were

205 generated using the "random" parameter, and data were split into 75% training and 25%

validation sets, ensuring a constant ratio of presence to pseudo-absence points in both datasets. Each model was run 10 times. The ensemble model was constructed using a weighted average approach, including only individual models with TSS ≥ 0.7 (Ricklin et al., 2018). Based on the simulated habitat suitability, species distribution areas were classified into "suitable" and "unsuitable" habitats using the threshold corresponding to the maximum TSS value (Zhang et al., 2022). Finally, the binarized results of all species were overlaid to generate a species richness distribution map of annual plants. To assess model predictive performance, this study used AUC and TSS as the main evaluation metrics. The AUC value reflects the model's ability to distinguish between presence and absence areas, ranging from 0 to 1, where 0.6–0.9 indicates moderate performance and 0.9–1.0 indicates excellent performance. TSS (True Skill Statistic) measures the consistency between sample data and model predictions, calculated as the difference between sensitivity and the false positive rate (1 - specificity), ranging from -1 to 1, where 0.4–0.85 indicates moderate performance and 0.85–1 indicates excellent performance (Liu & Guo, 2024).

### 2.4. Geometric Centroid Migration of Ephemeral Plant Species Richness

Species richness distribution maps were divided using the equal interval method in ArcGIS, where 0–10 represents low richness, 11–19 represents medium richness, and 20–29 represents high richness. This study investigates the centroid shifts of raster units with high ephemeral plant richness under current and 2050s time periods across different climate emission scenarios, aiming to explore the response of the

227 center of ephemeral plant richness in the Gurbantunggut Desert to climate change.
228 Taking the current period centroid of ephemeral plant richness in the Gurbantunggut
229 Desert as a reference, the positions of the richness centroids under different climate
230 emission scenarios in the 2050s are compared. A migration map of the richness
231 centroids from the present to the future period is generated, and the distances of the
232 migration routes are calculated.

233 **2.5. Migration Dynamics of Ephemeral Plant Species Richness**

234 To assess the migration dynamics of ephemeral plant species richness under
235 climate change in the Gurbantunggut Desert, this study quantified the immigration,
236 emigration, and persistence of ephemeral plant species within individual grid cells
237 under different future climate scenarios. The analyses were performed using the
238 species gain rate (PSG), species loss rate (PSL), and species turnover rate (PST) as
239 quantitative metrics (Thuiller et al., 2005).

240 Species gain rate (PSG) represents the percentage of newly added (gained)
241 species from time point T1 to T2 relative to the total number of species at time point
242 T1. A higher PSG indicates a greater magnitude of species colonization within an
243 individual grid cell. The calculation formula is as follows:

244 $$PSG = \frac{G}{R} \times 100\%$$

245 Here, PSG denotes the species gain rate, G represents the number of species
246 gained within a grid cell from the current period to the 2050s, and R is the species
247 richness under the climatic conditions of the current period.

Species loss rate (PSL) represents the percentage of species that disappear (are lost) from time T1 to T2 relative to the total number of species at time T1. A higher PSL indicates a greater magnitude of species loss or outward migration within a given grid cell. The formula is as follows:

$$PSL = \frac{L}{R} \times 100\%$$

PSL denotes the species loss rate, L is the number of species lost within a grid cell from the current period to the 2050s, and R is the species richness under current climatic conditions.

Species turnover (PST) is calculated based on the number of species lost (L) and gained (G) per raster cell between two time points, in relation to the species richness of the current period. A higher PST indicates a greater compositional change within the raster cell. The calculation formula is as follows:

$$PST = \frac{(L+G)}{(G+R)} \times 100\%$$

Here, PST represents the species turnover rate; L denotes the number of species lost in a raster cell from the current period to the 2050s; G denotes the number of species gained in a raster cell over the same period; and R represents the species richness under the climatic conditions of the current period.

In this study, the aforementioned migration and change analyses were primarily conducted using ArcGIS software.

## 2.6. Geographically Weighted Regression Analysis of Environmental Factors *Affecting the Richness of Short-Lived Plants*

Before conducting geographically weighted regression (GWR) analysis, it is necessary to examine whether the species richness of short-lived plants exhibits significant spatial clustering (Chen, 2009). In this study, the global Moran's I index was employed to assess spatial autocorrelation. The index ranges from -1 to 1, where a significantly positive value indicates clustering of high values adjacent to high values and low values adjacent to low values, a significantly negative value indicates a dispersed pattern of high and low values, and a value close to zero suggests a near-random distribution. To further clarify local spatial association patterns, the local Moran's I index was used to generate a LISA cluster map, classifying clustering types into high–high, low–low, low–high, high–low, and non-significant regions.

Geographically Weighted Regression (GWR) is a classical spatial local regression model that can characterize the spatial heterogeneity of relationships between variables, overcoming the limitation of traditional global regression which assumes constant relationships (Yang et al., 2022). In this study, twelve environmental factors were used as independent variables, and the species richness of short-lived plants was treated as the dependent variable. A GWR model was constructed using GWR 4.0 software to analyze the spatial differentiation of the effects of environmental factors on species richness.

### 2.7. Calculation of Climate Velocity

In this study, the distance-based climate velocity was calculated using the k-nearest neighbors (KNN) algorithm. The core procedure is as follows: first, climate

raster values for the current and future periods were extracted to quantify climatic similarity; for each current-period climate raster, the KNN algorithm was employed to identify the most similar future-period raster; finally, the ratio of the geodesic distance between the current raster and its most similar future raster to the time interval represents the climate velocity. The calculation formula is as follows (Dobrowski & Parks, 2016):

$$V = \frac{d}{\Delta time}$$

In the formula, VVV denotes climate velocity (km/yr); ddd is the geodesic distance between the current raster and the most similar future raster (km); and Δtime\Delta timeΔtime is the temporal interval between the two periods (years).

The above climate velocity calculations were implemented using the "RANN" package in R, based on six climatic variables (Bio2, Bio9, Bio11, Bio13, Bio14, and Bio16) from the ephemeral plant species richness simulation. The temporal span ranged from the current period to the 2050s, encompassing four climate scenarios: SSP1-2.6, SSP2-4.5, SSP3-7.0, and SSP5-8.5.

### 2.8. Optimization of Priority Conservation Areas

The Zonation model is a spatial prioritization tool that supports multiple cost constraints. Based on the marginal loss principle, it iteratively removes the landscape units with the lowest conservation value and recalculates the priority of the remaining units until the ranking stabilizes, ultimately producing a continuous nested landscape sequence with values ranging from 0 to 1 (Shen et al., 2024).

In this study, Zonation 5 v2.3 was used, with the algorithm set to CAZ2. First, short-lived plant species richness was used as the feature layer. For the current period, cost layers were not considered, whereas for future periods, climate velocity was used as the cost layer (with cost weights based on the contribution of environmental factors in the ensemble model). The model was run to obtain a core conservation area ranking map, which was classified into high, medium, and low levels using the natural breaks method in ArcGIS. Second, species loss under future climate scenarios was used as the feature layer, with climate velocity as the cost layer. Using the same method, a key risk area ranking map was produced and similarly classified into high, medium, and low levels.

Finally, the ranking maps of core conservation areas and key risk areas were overlaid through raster algebra. Based on the classification criteria in Table 2, primary, secondary, and tertiary priority conservation areas for short-lived plants in the Gurbantunggut Desert were delineated.

**Table 2.** Classification Criteria for Priority Conservation Areas of Short-Lived Plants in the Gurbantunggut Desert

| | Core Conservation Area | Key Risk Area |
|---|---|---|
| Primary Priority Area | High | High |
| Secondary Priority Area | High | Medium |
| | Medium | High |
| Tertiary Priority Area | Medium | Medium |

# 3. Results

## 3.1. Accuracy Assessment of Short-Lived Plant Species Distribution Modeling

The ecological niche models developed in this study exhibited high accuracy in simulating the distribution of short-lived plant species, with the potential distribution ranges of each species showing strong agreement with their actual distributions, indicating that the model outputs are reliable and reasonable. Among all modeled species, 22 species (accounting for 62.85%) had AUC values greater than 0.9 and TSS values exceeding 0.85, indicating excellent model performance. Notably, species such as *Arnebia decumbens* (AUC = 0.999, TSS = 0.995) and *Isatis minima* (AUC = 0.998, TSS = 0.99) showed particularly outstanding simulation accuracy, whereas a few species, including *Schismus arabicus* (AUC = 0.863, TSS = 0.717), exhibited moderate accuracy (Table. 3). Overall, the ensemble models constructed in this study demonstrated robust predictive performance.

**Table 3.** AUC and TSS Values of Distribution Model Simulations for Short-Lived Plant Species

| Family | Species | AUC | TSS |
|---|---|---|---|
| Brassicaceae | *Lepidium perfoliatum* | 0.94 | 0.9 |
| | *Alyssum dasycarpum* | 0.974 | 0.876 |
| | *Malcolmia scorpioides* | 0.972 | 0.863 |
| | *Isatis violascens* | 0.893 | 0.808 |
| | *Tetracme quadricornis* | 0.924 | 0.853 |
| | *Malcolmia africana* | 0.874 | 0.75 |

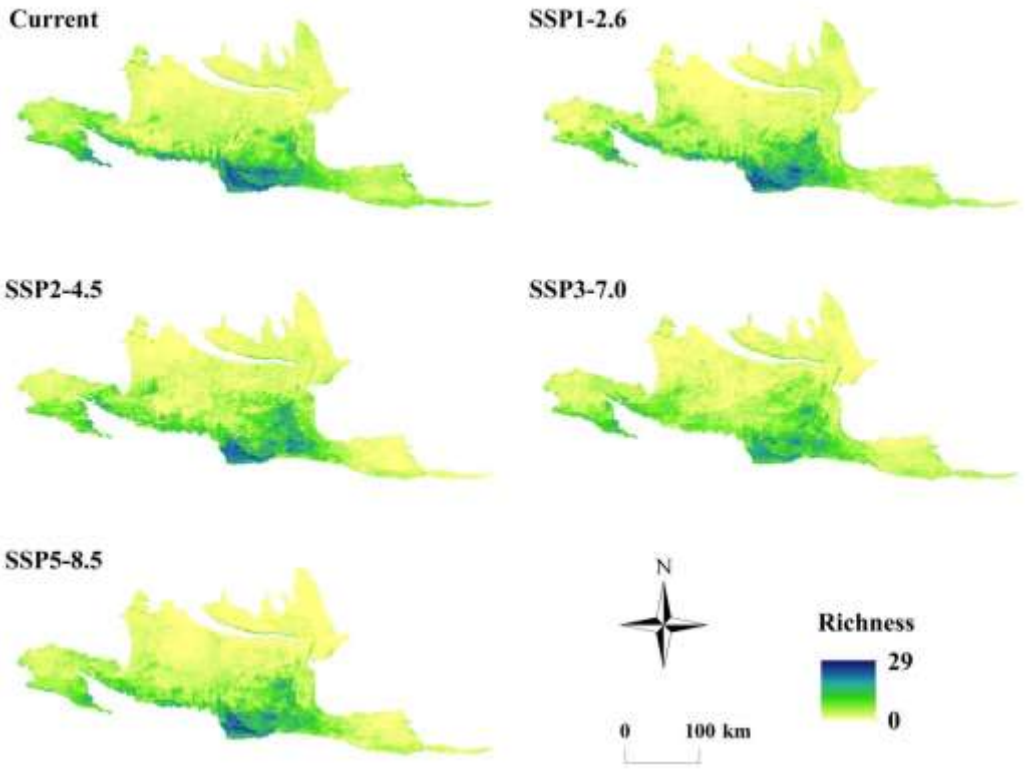
| | | | |
|---|---|---|---|
| | *Alyssum desertorum* | 0.996 | 0.987 |
| | *Alyssum linifolium* | 0.925 | 0.812 |
| | *Tetracme recurvata* | 0.928 | 0.812 |
| | *Isatis minima* | 0.998 | 0.99 |
| Boraginaceae | *Nonea caspica* | 0.976 | 0.889 |
| | *Lappula semiglabra* | 0.977 | 0.865 |
| | *Arnebia decumbens* | 0.999 | 0.995 |
| Gramineae | *Schismus arabicus* | 0.863 | 0.717 |
| | *Eremopyrum orientale* | 0.924 | 0.726 |
| | *Bromus tectorum* | 0.956 | 0.854 |
| | *Eremopyrum distans* | 0.989 | 0.97 |
| Compositae | *Hyalea pulchella* | 0.934 | 0.775 |
| | *Senecio subdentatus* | 0.918 | 0.706 |
| | *Garhadiolus papposus* | 0.974 | 0.952 |
| | *Koelpinia linearis* | 0.973 | 0.939 |
| | *Heteracia szovitsii* | 0.994 | 0.988 |
| Chenopodiaceae | *Corispermum lehmannianum* | 0.966 | 0.869 |
| | *Ceratocarpus arenarius* | 0.961 | 0.801 |
| Geraniaceae | *Erodium oxyrrhynchum* | 0.939 | 0.731 |
| Papaveraceae | *Hypecoum erectum* | 0.987 | 0.971 |
| | *Hypecoum parviflorum* | 0.997 | 0.989 |
| Liliaceae | *Eremurus inderiensis* | 0.973 | 0.871 |

| | | | |
|---|---|---|---|
| | *Eremurus anisopterus* | 0.993 | 0.981 |
| Leguminosae | *Astragalus arpilobus* | 0.983 | 0.959 |
| | *Trigonella arcuata* | 0.929 | 0.805 |
| Cyperaceae | *Carex physodes* | 0.986 | 0.878 |
| Plantaginaceae | *Plantago minuta* | 0.941 | 0.781 |
| Lamiaceae | *Ne*peta micra*ntha* | 0.952 | 0.846 |
| *Apiaceae* | Soranthus meyeri | 0.976 | 0.923 |

### 3.2. Spatial Patterns of Annual Plant Species Richness

Currently, the species richness of annual plants exhibits an overall spatial pattern characterized by higher values in the south and west and lower values in the north and east, with hotspots primarily distributed along the transitional zones between deserts and oases that receive seasonal water input (Figure. 3). Under all climate scenarios projected for the 2050s, the average species richness is expected to decline, with the magnitude of reduction positively correlated with the intensity of greenhouse gas emissions, and the spatial pattern is predicted to change markedly. Under the SSP1-2.6 scenario, the decline in average species richness is minimal, and the distribution pattern remains similar to the present, suggesting that communities can maintain relative stability under climate mitigation strategies. In contrast, under the SSP2-4.5, SSP3-7.0, and SSP5-8.5 scenarios, the hotspots of species richness contract noticeably, particularly in the southern desert, with the lowest average species richness occurring under the SSP5-8.5 scenario. Overall, future climate change is

projected to lead to a general decrease in the species richness of annual plants, with a significant contraction of southern hotspots. If climate continues to trend toward higher temperatures and increased aridity, early-spring annual plant diversity will face severe threats.



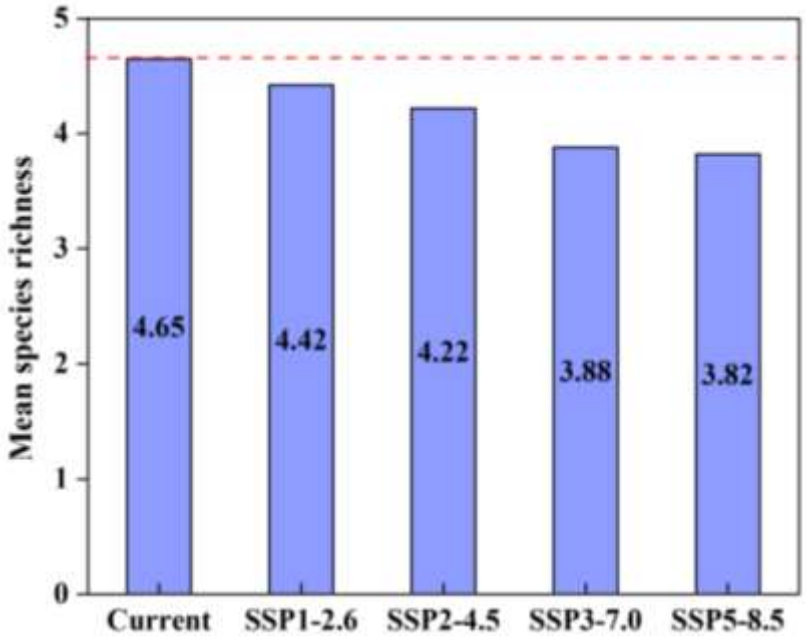



**Figure 3.** Ephemeral plant species richness distribution in Gurbantunggut Desert under current and 2050s climate scenarios

The latitudinal and longitudinal distribution patterns of mean species richness of ephemeral plants in the Gurbantunggut Desert under the current and 2050s scenarios indicate (Figure. 4) that along the longitudinal gradient, the scenario curves largely overlap within the 86°E–89°E range, whereas notable differences are observed on both the eastern and western flanks. Along the latitudinal gradient, the scenario curves exhibit a "gradual fluctuation–rapid increase–rapid decline" pattern, with peak values occurring between 45.8°N and 46.0°N. In both longitudinal and latitudinal directions, the mean species richness under all 2050s scenarios shows a declining trend compared to the current conditions.

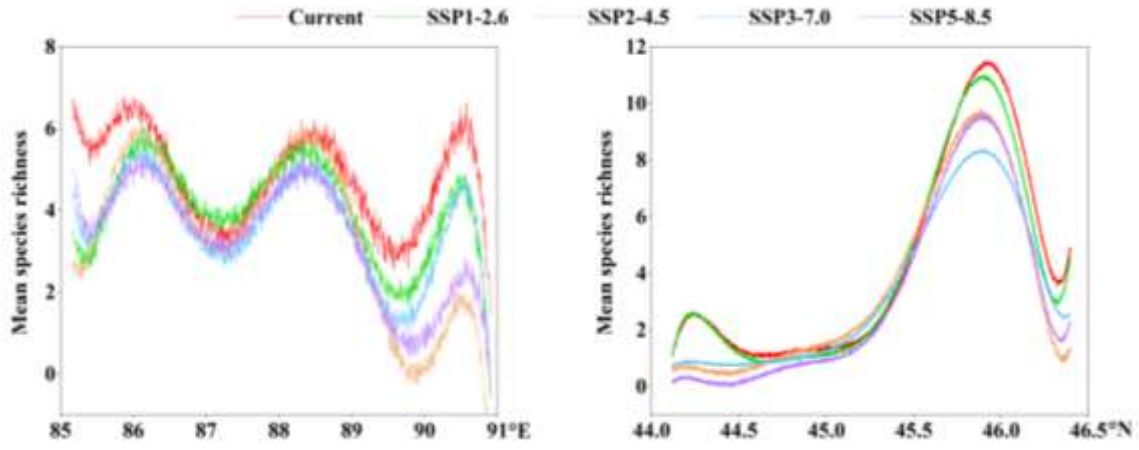



**Figure 4.** Latitudinal and longitudinal gradients of ephemeral plant richness in Gurbantunggut Desert under current/2050s climates.

## 3.3. Environmental Drivers of Ephemeral Plant Richness Based on Geographically Weighted Regression

At present, the global Moran's I index for ephemeral plant richness in the

Gurbantunggut Desert is 0.91 ($p < 0.01$), with a z-score of 315.29, indicating a highly significant spatial clustering pattern. Regarding local clustering types, "high–high" and "low–low" patterns dominate: the former is concentrated in the southern part of the desert, while the latter is mainly distributed in the northern part (Figure. 5).

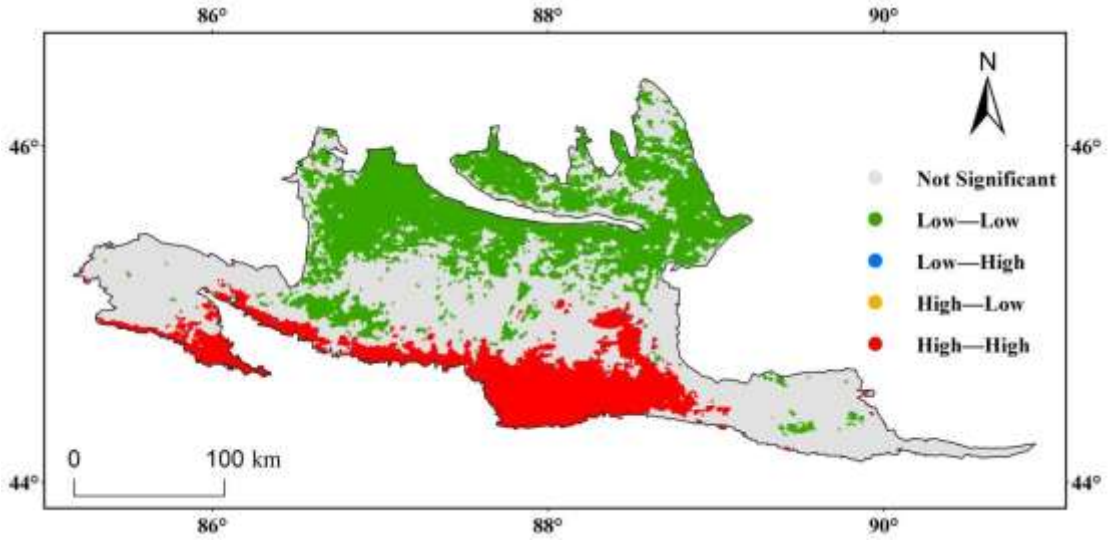



**Figure 5.** Local Spatial Autocorrelation (LISA) Distribution of Ephemeral Plant Species Richness in the Gurbantünggüt Desert

Geographically Weighted Regression (GWR) analysis indicated that the effects of environmental variables on the species richness of ephemeral desert plants exhibited significant spatial heterogeneity (Figure. 6). Soil clay content (CC), pH, silt content (SC), soil organic carbon (SOC), and precipitation of the wettest month (Bio13) primarily exerted inhibitory effects, whereas snow-free days (SF), snow onset date (ST), mean temperature of the coldest quarter (Bio11), precipitation of the driest month (Bio14), precipitation of the wettest quarter (Bio16), mean diurnal temperature range (Bio2), and mean temperature of the driest quarter (Bio9) mainly showed positive driving effects.

Specifically, the impacts of individual environmental factors on species richness displayed pronounced spatial differentiation. Soil factors: clay content (CC) was significantly positively correlated at the eastern margin of the desert, while negative correlations were observed in the central and western regions; pH was significantly negatively correlated at the southern margin and shifted to positive correlation in the northern margin; silt content (SC) showed positive correlation in parts of the northern desert and significant negative correlation along the western margin; SOC exhibited negative correlation across most desert regions. Snow-related factors: snow-free days (SF) were negatively correlated in the northern desert but became positively correlated in parts of the southern region; snow onset date (ST) showed positive correlation in the central-southern desert and negative correlation in the north. Temperature factors: mean temperature of the coldest quarter (Bio11) displayed positive correlation concentrated in the southern desert, whereas negative correlations were sporadically distributed without clear clustering; mean diurnal temperature range (Bio2) was significantly positively correlated in the central-southern desert, but shifted to negative correlation along the northern and western margins; mean temperature of the driest quarter (Bio9) was positively correlated in the central-southern desert and negatively correlated in the western, northern, and eastern regions. Precipitation factors: precipitation of the wettest month (Bio13) was negatively correlated across the entire desert; precipitation of the driest month (Bio14) showed positive correlation along the southern margin and negative correlation elsewhere; precipitation of the wettest quarter (Bio16) was consistently positively

correlated across all regions.

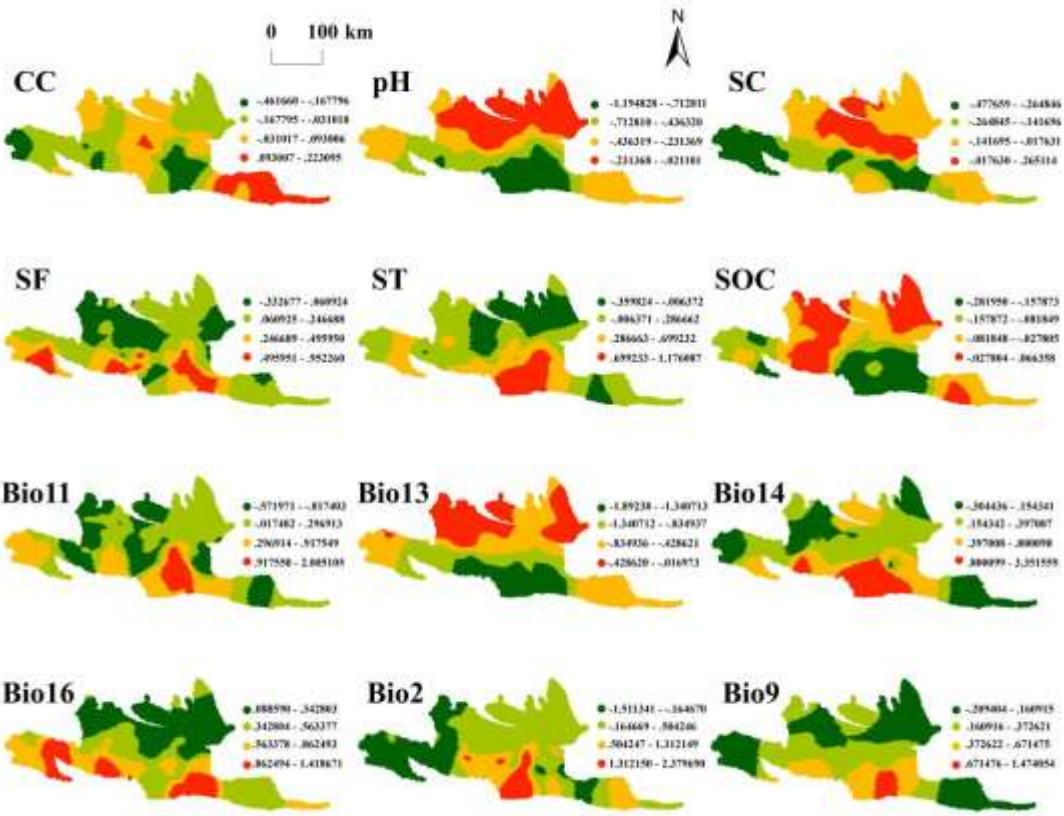



**Figure 6.** Spatial distribution of standardized regression coefficients of each variable in GWR model for species richness.

### 3.4. Centroid Shifts of Short-lived Plant Species Richness

By the 2050s, under all climate scenarios, the centroids of high species richness exhibited noticeable shifts, showing an overall tendency to move toward the southeastern part of the desert (Figure. 7). Under the SSP1-2.6 scenario, the centroid shifted approximately 8.36 km eastward; under the SSP2-4.5 and SSP3-7.0 scenarios, the centroids both shifted southeastward, with distances of 14.62 km and 12.55 km, respectively; under the SSP5-8.5 scenario, the centroid shifted 7.94 km, with the direction tending further south.

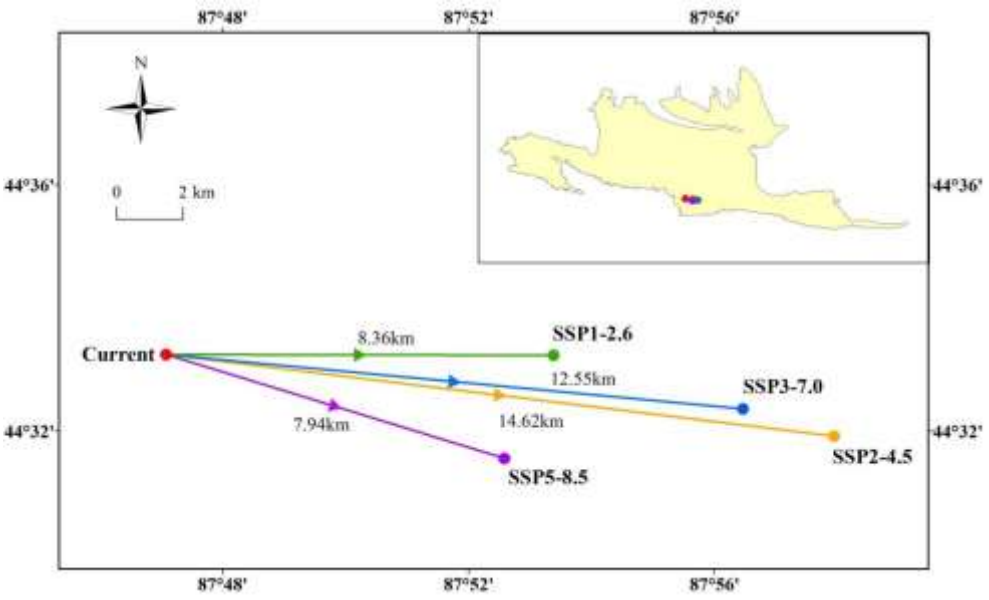
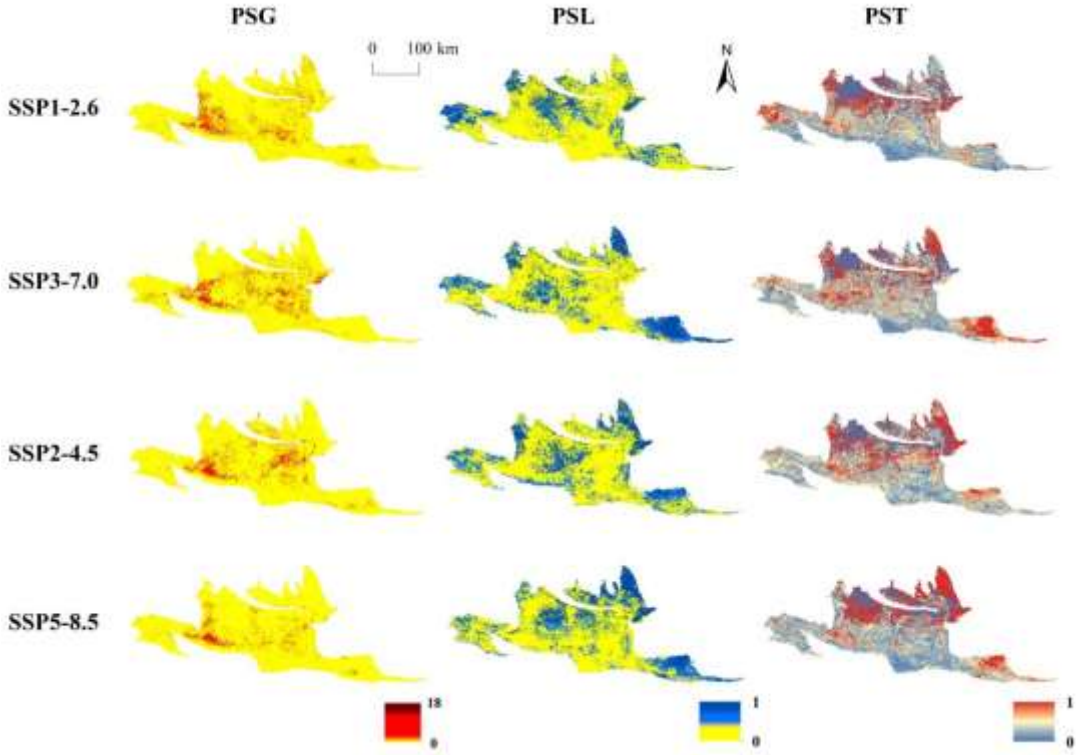



**Figure 7.** Centroid shifts of high-richness ephemeral plant areas in Gurbantunggut Desert under current and 2050s climate.

Overall, the spatial patterns of species gain rate (PSG), loss rate (PSL), and turnover rate (PST) exhibited significant heterogeneity (Figure. 8). High PSG areas were fragmented and primarily distributed in the central desert, and as the scenario shifted from SSP1-2.6 to SSP5-8.5, the extent of these high-value areas showed a contracting trend, indicating that future climate change may transform some currently unsuitable habitats into suitable ones. High PSL areas were mainly located at the desert margins and certain central regions, and with increasing scenario intensity, both the range and magnitude of these areas expanded, corroborating the conclusion of low-richness expansion and medium-to-high richness reduction, suggesting decreased habitat suitability and elevated local extinction risk in the aforementioned regions. High PST areas were concentrated in the northern desert, reflecting more active species composition turnover and unstable community structure. Notably, under SSP3-7.0 and SSP5-8.5 scenarios, the extent of high PST areas markedly expanded,

indicating that more severe climate change intensifies species reassembly and community dynamics fluctuations.

As scenarios progressed from SSP1-2.6 to SSP5-8.5, PSG first increased and then decreased, reaching its peak under the SSP2-4.5 scenario; PSL continued to rise; and PST remained higher than the SSP1-2.6 level across all scenarios.



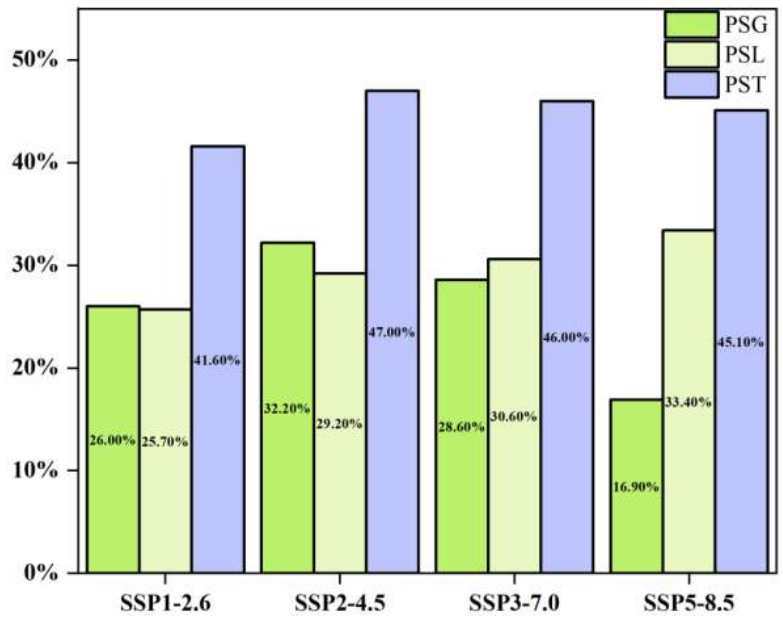
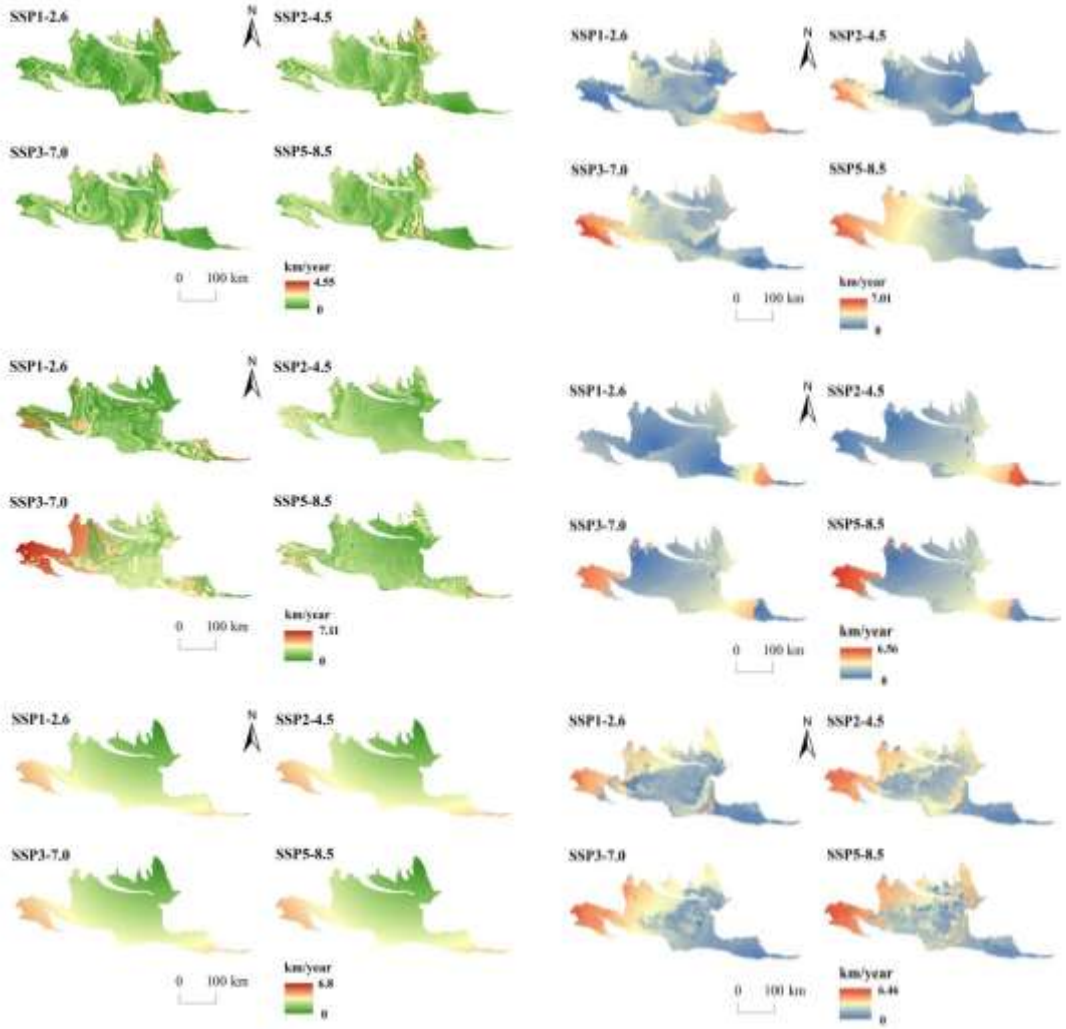



**Figure 8.** Spatial distribution of PSG, PSL, PST (ephemeral plants) in Gurbantunggut Desert under current/2050s climates.

### 3.5 Spatial Patterns of Climate Velocity

Climate velocity represents the rate of spatial change of climatic factors, and its spatial patterns reflect the heterogeneity of regional climate variability. Under different climate scenarios in the 2050s, the climate velocity of temperature and precipitation factors exhibits distinct spatial differentiation patterns (Figure. 9). For temperature factors, high-value areas of Bio2 are sporadically distributed along the northern edge of the desert, with minimal differences among scenarios; high-value areas of Bio9 are scattered under SSP1-2.6 and SSP2-4.5 scenarios, whereas under SSP3-7.0, a distinct high-value aggregation appears in the western desert, and under SSP5-8.5, it further contracts. For precipitation factors, high-value areas of Bio11 are concentrated in the western desert across all scenarios, with no significant inter-scenario differences; high-value areas of Bio13 are mainly located in the eastern desert under SSP1-2.6, but shift to the western desert under SSP2-4.5, SSP3-7.0, and SSP5-8.5; high-value areas of Bio14 are sporadically distributed along the eastern desert margin under SSP1-2.6 and SSP2-4.5, while they move to the western margin under SSP3-7.0 and SSP5-8.5; high-value areas of Bio16 are consistently concentrated in the western desert across all scenarios, and their extent shows a clear expansion trend as scenarios progress toward SSP5-8.5. In terms of mean climate velocity, Bio2 (0.87–1.19 km/year) is lower than other factors, whereas Bio11, Bio13,

and Bio16 are generally higher. Notably, Bio9 under SSP3-7.0 is exceptionally prominent, indicating enhanced climate variability in this scenario; differences of Bio11 among scenarios are minor; Bio13 under SSP2-4.5 exhibits a markedly lower climate velocity; and the mean climate velocities of Bio14 and Bio16 gradually increase with scenario intensity.



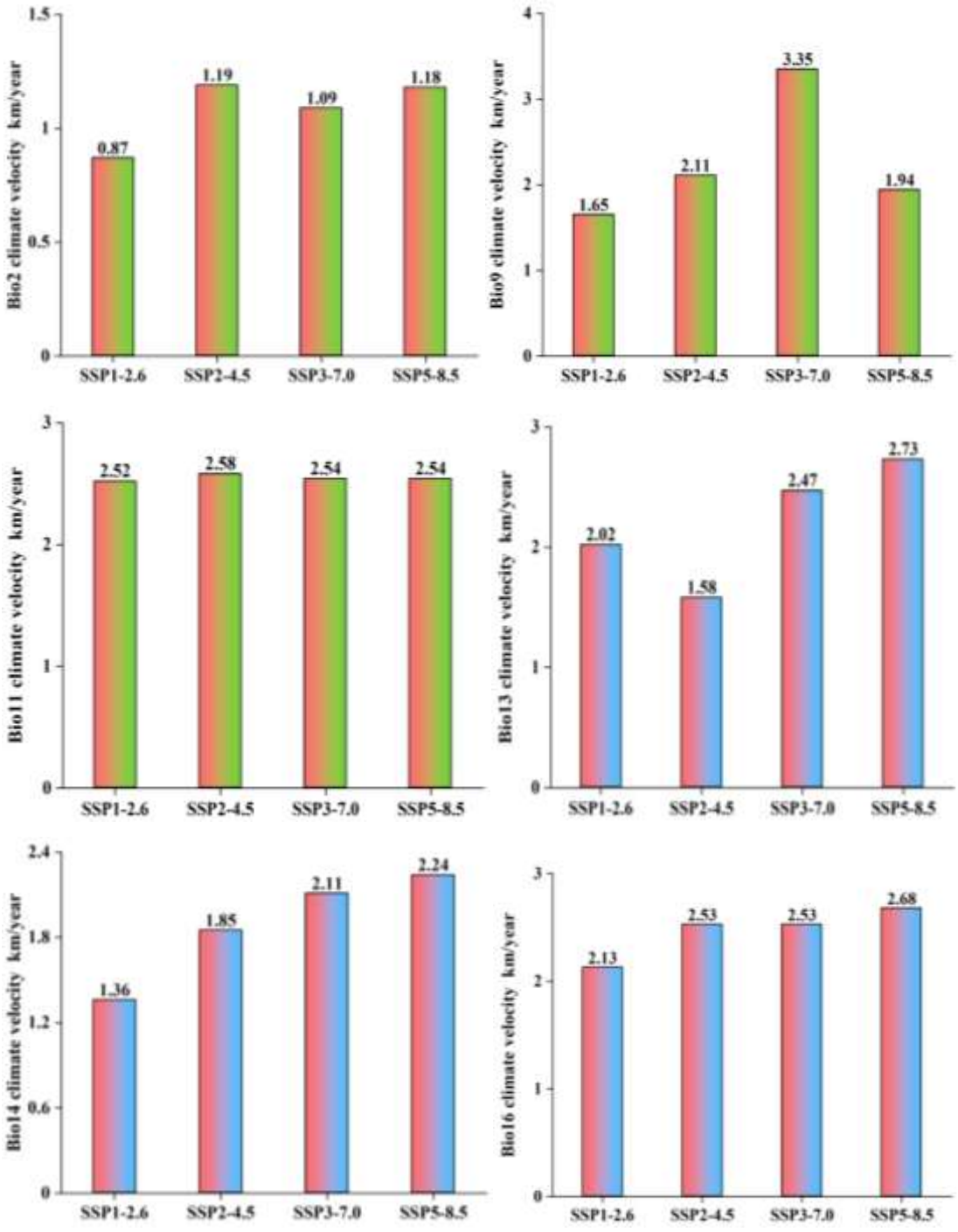
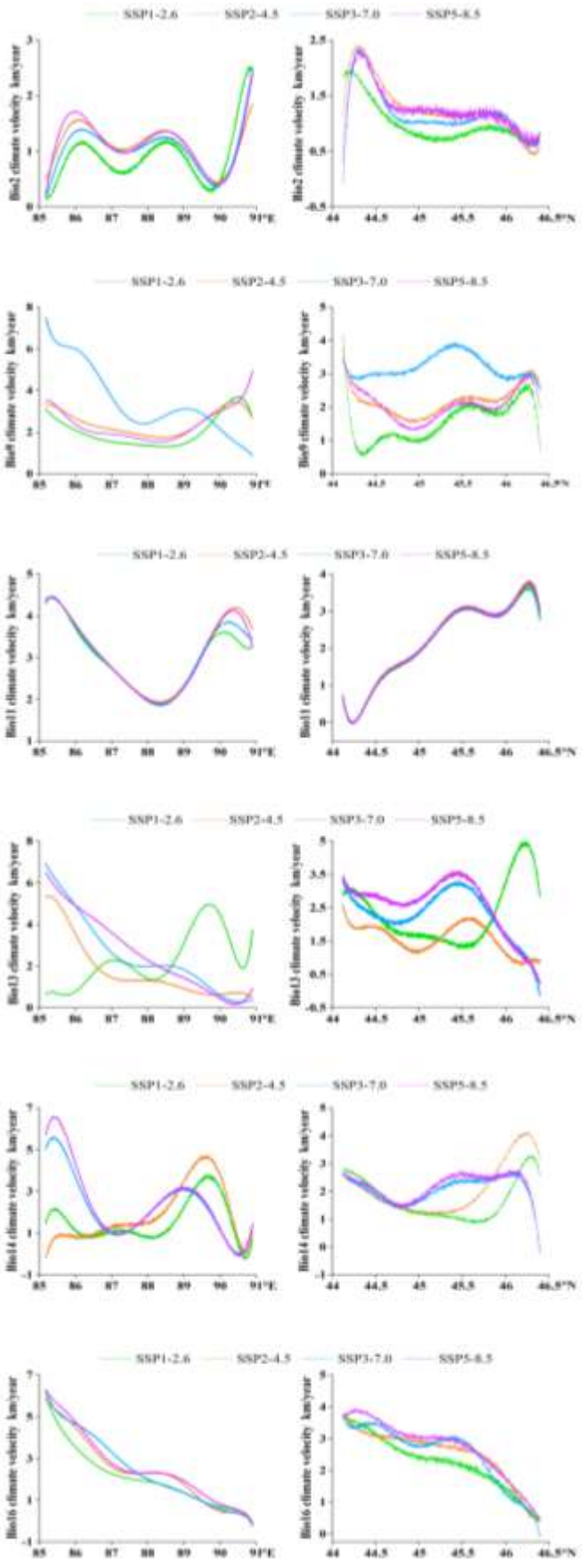



**Figure 9.** Spatial patterns of climate velocity of environmental variables under different climate scenarios in the 2050s.

Under different SSP scenarios, the climate velocities of various climatic factors exhibited pronounced spatial heterogeneity along both longitudinal and latitudinal gradients (Figure. 10). Along the longitudinal gradient, Bio2 showed a fluctuating

increasing trend under all scenarios; Bio9 exhibited an increasing trend under all scenarios except SSP3-7.0, where it decreased; Bio11 displayed a pattern of initial decline followed by subsequent increase; Bio13 generally decreased under all scenarios except SSP3-7.0, which showed an increasing trend; Bio14 exhibited a multi-peak fluctuating trend; and Bio16 consistently decreased under all scenarios. Along the latitudinal gradient, Bio2 showed an initial increase followed by a decrease under all scenarios; Bio9 fluctuated most mildly under SSP3-7.0; Bio11 continuously increased under all scenarios; Bio13 fluctuated upward under SSP3-7.0 but fluctuated downward under the other scenarios; Bio14 fluctuated upward under SSP1-2.6 and SSP2-4.5, but fluctuated downward under SSP3-7.0 and SSP5-8.5; and Bio16 consistently decreased under all scenarios.




497

498 **Figure 10.** Latitudinal and longitudinal distribution of environmental climate velocity under 2050s

scenarios

### 3.6. Optimization of Priority Conservation Areas for Short-lived Plants

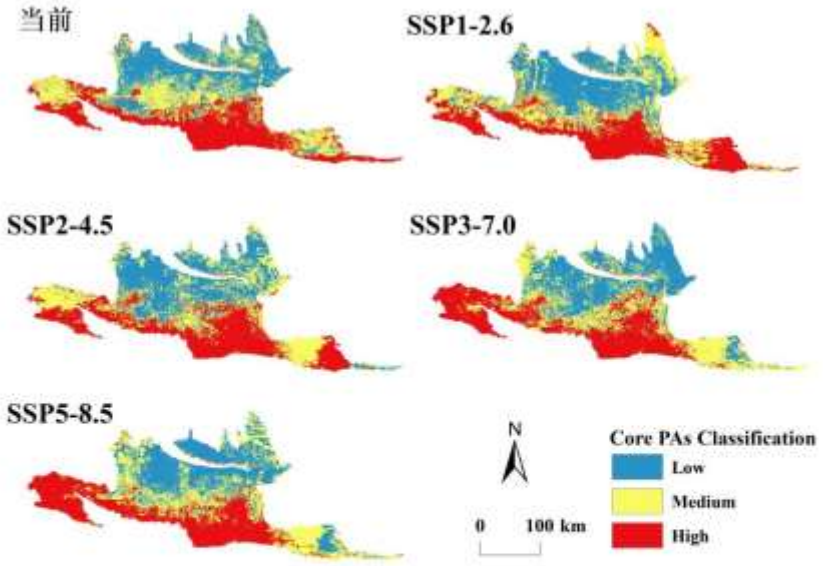
The core conservation areas for short-lived plants in the study region are mainly distributed in regions with relatively high current species richness and stable climatic velocities. At present, high-grade core conservation areas are concentrated in the southern part of the desert. By the 2050s, under all climate scenarios, their extent is projected to contract slightly, particularly in the western and eastern parts of the desert, indicating that severe climate change may undermine the ecological stability of existing core conservation areas (Figure. 11).

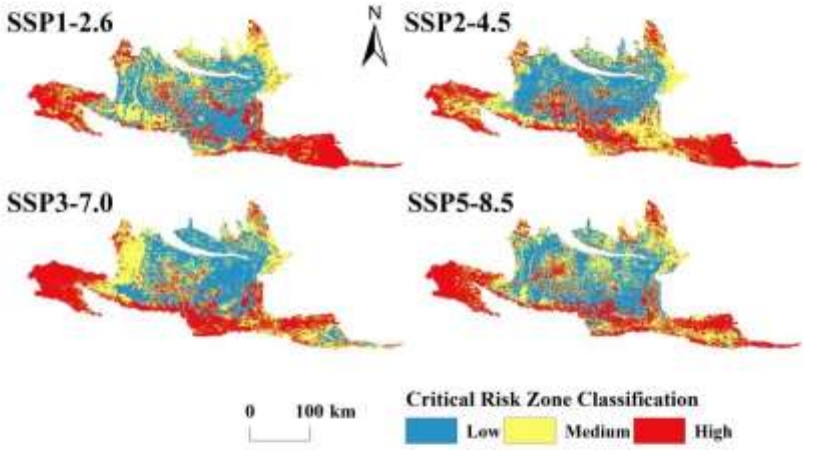
In the 2050s, high-risk zones under different climate scenarios are primarily located in the central, eastern, and western parts of the desert. Specifically, under the SSP1-2.6 and SSP2-4.5 scenarios, these zones are concentrated in fragmented areas of the desert center and west as well as the eastern desert; under the SSP3-7.0 and SSP5-8.5 scenarios, they are distributed across fragmented patches in the central and eastern desert and the western desert (Figure. 11).

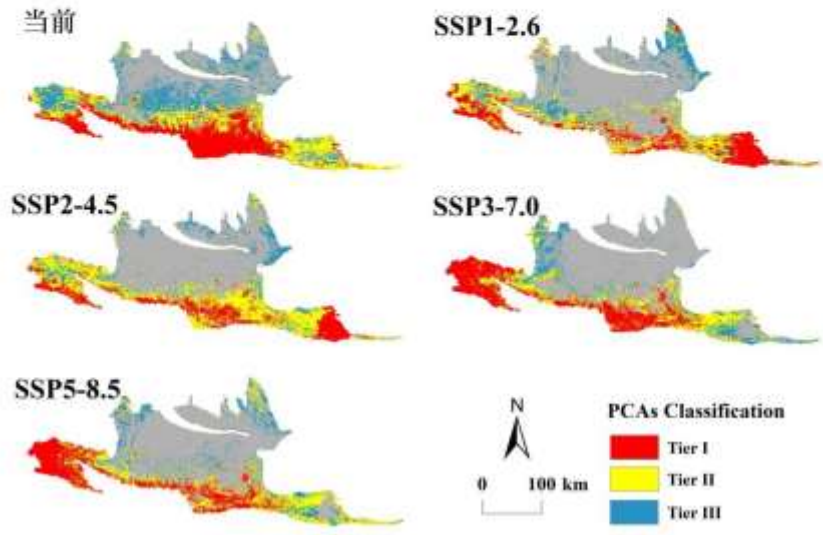
By integrating species diversity with loss risk, this study identified hierarchical priority conservation areas (Figure. 11). Currently, first-level priority areas are mainly located in the southern desert, covering a total area of $0.701 \times 10^4$ km². By the 2050s, under the SSP1-2.6 and SSP2-4.5 scenarios, first-level southern priority areas are projected to shrink significantly and shift eastward, with a notable reduction in total area; under the SSP3-7.0 and SSP5-8.5 scenarios, the southern first-level priority

areas experience slight shrinkage and shift westward, with a marked decrease in area as well.

Overall, current priority conservation areas for short-lived plants are mainly distributed in the southern, western, and eastern parts of the desert, covering a total area of $2.103 \times 10^4$ km². In the 2050s, the spatial pattern of conservation areas exhibits dynamic adjustments under different scenarios: under SSP1-2.6 and SSP2-4.5, they are mainly located at the southern edge of the desert center, the western, and eastern desert, with areas of $1.512 \times 10^4$ km² and $1.578 \times 10^4$ km², respectively; under SSP3-7.0 and SSP5-8.5, they are concentrated at the southern edge of the desert center and the western desert, covering $1.482 \times 10^4$ km² and $1.478 \times 10^4$ km², respectively. These results indicate that under different climate emission scenarios, the conservation patterns and risk distributions for short-lived plants exhibit pronounced dynamic responses.


当前
SSP1-2.6
SSP2-4.5
SSP3-7.0
SSP5-8.5
N
0 100 km
Core PAs Classification
Low
Medium
High


SSP1-2.6
N
SSP2-4.5
SSP3-7.0
SSP5-8.5
0 100 km
Critical Risk Zone Classification
Low
Medium
High


当前
SSP1-2.6
SSP2-4.5
SSP3-7.0
SSP5-8.5
N
0 100 km
PCAs Classification
Tier I
Tier II
Tier III

533

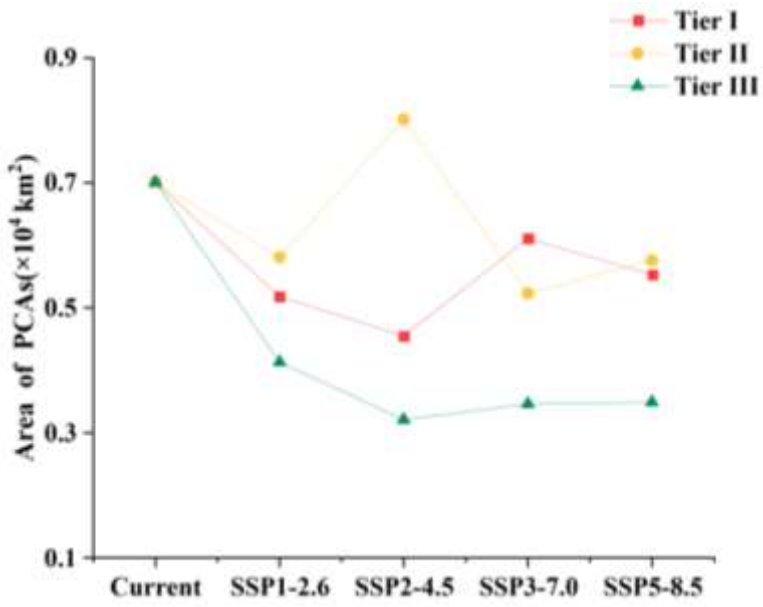



**Figure 11.** Spatial distribution of ephemeral plant core conservation areas, key risk areas, and priority conservation areas in the Gurbantunggut Desert under current and 2050s climate scenarios.

## 4. Discussion

### 4.1. Response of Ephemeral Plant Species Richness Patterns to Climate Change and Migration Characteristics

According to this study, under all climate scenarios by the 2050s, species richness of ephemeral plants in the study area exhibits a general pattern characterized by a contraction of southern hotspots and a decline in mean richness. With increasing carbon emission scenarios, the magnitude of richness reduction intensifies: under the SSP5-8.5 scenario, mean species richness is projected to decrease from the current 4.65 to 3.82, representing a relative decline of 17.8% (Figure. 3). This result provides quantifiable empirical evidence for understanding the impacts of climate change on

548 the diversity of desert-specific herbaceous layers. Previous studies have indicated that
549 climate-driven shifts in wet–dry patterns can lead to systematic changes in vegetation
550 structure and species composition in desert ecosystems (Huang et al., 2016; IPCC,
551 2022), thereby driving spatial reorganization of plant diversity. Over the past decades,
552 sustained spring warming in the Gurbantunggut Desert has intensified soil water
553 evapotranspiration, while concurrent precipitation and snowmelt supply have not
554 correspondingly increased, leading to an imbalance in regional water budgets (Chen et
555 al., 2019). This change imposes habitat aridification stress on ephemeral plants that
556 rely on brief spring moisture periods, highlighting their high sensitivity to water
557 availability and explaining the observed decline in species richness under warming
558 conditions. Alterations in regional hydrothermal patterns have generally reduced
559 habitat suitability for species, thereby weakening the ecosystem's capacity to maintain
560 diversity (IPCC, 2022). This finding is consistent with global assessments of
561 biodiversity decline (Işlar, 2019) and underscores the vulnerability of arid ecosystems,
562 in which even minor climatic disturbances can trigger disproportionately large
563 ecological deterioration (Berdugo et al., 2020).

564 Further analysis revealed that ephemeral plant diversity faces a dual climate
565 stress: not only is there an overall decline in species richness, but the spatial
566 distribution pattern is also projected to undergo significant restructuring. The centers
567 of high species richness are expected to shift toward the southeastern part of the desert,
568 with the maximum migration distance reaching 14.62 km under the SSP2-4.5 scenario
569 (Figure. 7). This migration pattern aligns with the expectations of the climate velocity

570 theory regarding species distributions in response to changing climatic conditions and
571 can be interpreted as the spatial response of ephemeral plants to suitable climatic
572 niches. The underlying mechanism can be explained from the perspective of "climatic
573 refugia" (Loarie et al., 2009): as the climate warms, the hydrothermal conditions in
574 the central desert become increasingly unfavorable, whereas the southeastern region
575 experiences relatively moderated warming due to topographic regulation and
576 maintains more stable snow cover and precipitation conditions (Zhang & Chen, 2002),
577 thereby forming refugial areas favorable for the persistence of ephemeral plants.

578 Species migration analysis further revealed that, by the 2050s under various
579 climate scenarios, the distribution of ephemeral plants exhibits pronounced regional
580 differentiation: the central desert is projected to become a net gain area for species
581 (with a fragmented distribution), whereas the northern and eastern regions are
582 identified as major loss areas and the zones experiencing the most intense species
583 composition changes (Figure. 8). The underlying mechanism for this pattern lies in
584 the alternating landforms of sand dunes and inter-dune plains in the central desert,
585 which facilitate the formation of localized micro-catchments. Under a warmer and
586 drier climate, these micro-catchments can still effectively retain spring snowmelt and
587 precipitation, maintaining relatively stable soil moisture conditions (Chen et al., 2019),
588 thereby providing species with suitable habitats that buffer against climate change. In
589 contrast, the desert margins are subjected to stronger climatic disturbances, potentially
590 exceeding the ecological tolerance thresholds of ephemeral plants, leading to habitat
591 contraction and pronounced changes in species composition.

592 The above changes in intensity were quantified using three indicators: by the
593 2050s, under increasing emission scenarios, the species gain rate (PSG) increased
594 from 16.9% to 26.0%, the species loss rate (PSL) rose from 28.6% to 33.4%, and the
595 species turnover rate (PST) increased from 41.6% to 47.0% (Figure. 8). This indicates
596 that intensified climate stress will significantly enhance the instability and dynamic
597 turnover of short-lived plant communities, a trend consistent with previous findings
598 that climate warming accelerates plant species turnover and community reassembly
599 (Wang et al., 2021).

600 Climate velocity analysis further revealed that different climatic factors exhibit
601 significantly distinct rates of future change in the Gurbantunggut Desert (Figure. 9).
602 Under the SSP5-8.5 scenario, the mean climate velocity of the mean temperature of
603 the coldest quarter (Bio11) reaches 2.73 km/yr, markedly higher than that of other
604 environmental variables, indicating the most rapid spatial migration of temperature
605 seasonality. As the mean temperature of the coldest quarter directly determines the
606 thermal conditions for the germination of ephemeral plants, its rapid change may
607 disrupt the synchrony between species phenology and environmental cues, thereby
608 affecting the successful completion of their life cycle (Liu et al., 2019). Meanwhile,
609 the mean climate velocity of precipitation in the wettest month (Bio13) under the
610 same scenario also reaches 2.73 km/yr, representing the most pronounced change
611 among precipitation-related variables. Its spatial migration reflects the redistribution
612 of moisture resources during the wet period, which will directly constrain water
613 availability during the critical growth stages of ephemeral plants.

Further analysis revealed that areas with high climatic velocity for precipitation factors (Bio13 and Bio14) were primarily located in the southern part of the desert, whereas high-value areas for temperature factors (Bio2 and Bio9) were concentrated in the northern part of the desert, indicating a clear spatial differentiation between the two (Figure. 9). This spatial heterogeneity of climatic velocity mechanistically explains why the centroid of future species richness distribution is expected to undergo region-specific shifts (Figure. 7), and provides critical scientific evidence for formulating differentiated species conservation strategies across distinct regions of the desert ecosystem.

### 4.2. Environmental Drivers of the Spatial Patterns of Ephemeral Plant Richness

This study employed a geographically weighted regression (GWR) model to reveal the spatially heterogeneous responses of ephemeral plant species richness to environmental factors. The results indicated that precipitation of the wettest quarter (Bio16) and precipitation of the driest month (Bio14) exerted the most significant positive driving effects, whereas soil pH and precipitation of the wettest month (Bio13) exhibited the most pronounced negative influences (Figure. 6). These findings corroborate the notion that ephemeral plants, as a typical water-dependent functional group, are geographically constrained by the availability of spring water in desert ecosystems, derived from snowmelt and precipitation. The above results not only support Noy-Meir's (1973) classical assertion that "water is the decisive limiting factor in arid ecosystems," but also, through the spatial differentiation of the

directions of key factor effects, reveal the complexity of water regulation mechanisms: the survival and reproduction of ephemeral plants depend not only on the total amount of water but also on the timing and intensity of precipitation relative to their critical phenological stages (Van Rooyen et al., 1992).

From the perspective of positive driving factors, this study confirms that Bio16 (precipitation of the wettest quarter) is the most important moisture-related factor influencing the richness of ephemeral plants. GWR analysis indicates that its positive effect peaks in the southern part of the desert and gradually weakens northward, exhibiting pronounced spatial heterogeneity. Specifically, in the southern desert, higher Bio16 values correspond to the critical precipitation period from spring to early summer, which closely aligns with the germination-to-reproduction phenological period of ephemeral plants in this region (Figure. 6), providing sufficient water to rapidly complete their life cycle (Yuan & Tang, 2010). This stable moist window directly shapes the spatial pattern of high species richness in the south and explains why this area may serve as a “climatic refuge” for ephemeral plant diversity in the future. Meanwhile, Bio14 (precipitation of the driest month) also demonstrates a key positive effect (Figure. 6). GWR results show that this factor is more pronounced in the central and western desert, providing a basis for explaining species persistence in sparsely distributed areas. Even under overall arid conditions, the minimal precipitation characterized by Bio14 in winter or early spring can effectively alleviate extreme surface soil drought, supplying the germination-required initial moisture for local species (Van Rooyen et al., 1992; Yuan & Tang, 2010). This is crucial for

ephemeral plants that must complete their life cycle within a short temporal window, offering a mechanistic explanation for why some sparsely distributed areas can maintain a certain level of species persistence under climate warming. Among negative environmental factors, the mechanisms of Bio13 (precipitation of the wettest month) and soil pH were further revealed (Figures 6 and 8). GWR analysis shows that the negative effect of Bio13 is most pronounced in the northern and eastern desert (Figure. 6), which correspond to the core zones of potential future species richness loss, highlighting the spatial aggregation of phenological mismatch risks. This finding not only aids in understanding the current spatial heterogeneity of ephemeral plant richness but also provides a critical mechanistic explanation for predicting their potential future loss areas.

The negative impact of Bio13 is highly consistent with the prediction that the northern and eastern parts of the study area represent the primary future loss zones for ephemeral plants (Figure. 8). The core of this negative effect lies in the mismatch between water availability and phenology: the wettest months of July–August coincide with the dormancy period of most ephemeral species, and precipitation events physically disrupt the fragile surface biological soil crust rather than being effectively utilized, exposing or displacing seeds and destroying the established seed bank, thereby affecting autumn population regeneration (Chen et al., 2021). These quantitative results confirm that the effectiveness of water must be precisely synchronized with the brief life-history window of plants; otherwise, periods of high moisture can paradoxically act as limiting factors. Similarly, the negative effect of soil

679 pH reveals another critical mechanism: the regional soil chemical environment and
680 water conditions jointly form a coupled “water–nutrient” limitation. GWR analysis
681 indicates that this negative effect is particularly pronounced in the northern and
682 eastern desert areas (Figure. 6), highlighting the spatial heterogeneity of soil chemical
683 constraints. In arid desert regions, slightly alkaline soils not only directly limit plant
684 growth by immobilizing nutrients such as phosphorus and suppressing microbial
685 activity, but also further reduce water-use efficiency under conditions of limited
686 moisture (Li et al., 2025). Therefore, the negative effect of pH acts synergistically
687 with water stress, providing a more comprehensive mechanistic explanation for the
688 distributional constraints of ephemeral plants in alkaline habitats. This coupled stress
689 mechanism is most prominent in the northern desert.

690 The GWR results indicate that the absolute value of the soil pH regression
691 coefficient in this region is significantly higher than in other areas, suggesting an
692 amplification of soil chemical constraints (Figure. 6). Specifically, the pedogenic
693 parent material is rich in carbonates, and strong evaporation drives the surface
694 accumulation of salts, jointly exacerbating the negative effects of high pH. This
695 combined “high pH–high salinity” effect fundamentally explains the persistently low
696 species richness in this region and predicts that it will face elevated ecological risks
697 (Azevedo et al., 2012).

698 In summary, phenological mismatches driven by Bio13 (precipitation of the
699 wettest month) combined with soil pH–mediated “water–nutrient” coupling stress
700 jointly constitute a constraining framework for understanding the distribution of

ephemeral plants. This framework not only elucidates the observed spatial pattern changes, such as the decline in species richness in the northern and eastern regions, but also provides a mechanistic basis for assessing and predicting community vulnerability under future climate scenarios.

### 4.3. Identification of Priority Conservation Areas for Ephemeral Plants and Implications for Adaptive Conservation

This study, based on a two-dimensional integrated framework of "centers of species diversity–future loss risk," innovatively combines the Zonation model with spatial overlay analysis to delineate priority conservation areas for short-lived plant diversity in the Gurbantunggut Desert. This approach simultaneously considers existing biodiversity hotspots and potential loss risks under future climate stress, addressing the limitation of traditional planning that focuses solely on current high-richness regions, and provides a more practical pathway for biodiversity conservation in arid regions.

From the perspective of spatiotemporal evolution, the current total area of priority conservation zones is approximately $2.10 \times 10^4$ km², primarily distributed in the southern, western, and eastern regions of the desert where water and thermal conditions are relatively stable (Figure. 11), which closely aligns with the “higher in the south and west, lower in the north and east” pattern of species richness in the study area (Figure. 3). By the 2050s, the area is projected to contract significantly under all scenarios (SSP1-2.6: $1.512 \times 10^4$ km²; SSP2-4.5: $1.578 \times 10^4$ km²; SSP3-7.0:

722 $1.482 \times 10^4$ km²; SSP5-8.5: $1.478 \times 10^4$ km²), accompanied by a reconfiguration of
723 spatial patterns: under low-stress scenarios, priority areas will aggregate toward the
724 southern margin of the central desert, as well as the western and eastern regions;
725 under high-stress scenarios, they will further contract to the southern central and
726 western areas (Figure. 11). This evolutionary response reflects the regional
727 heterogeneity of climate velocity in the study area and the southeastward migration
728 trend of the species richness centroid (Figure. 7).

729 From the perspective of conservation priority, primary protected areas for
730 short-lived plant species simultaneously encompass core areas of biodiversity and
731 regions at risk under future summer climate, representing irreplaceable conservation
732 priorities. Although these areas are relatively small, they possess the highest potential
733 for species persistence (Figure. 11). In practical conservation, habitat connectivity
734 within primary areas should be ensured by minimizing barriers to seed dispersal
735 caused by roads, irrigation channels, and grazing (Yang et al., 2022). To address
736 mismatches between water availability and phenology, simple water-harvesting
737 facilities can be established to enhance spring water supply, and local species can be
738 supplemented to aid restoration. Monitoring stations should also be set up to track
739 hydrothermal changes and population dynamics during critical phenological periods
740 of short-lived plants. Secondary protected areas function as buffer zones, primarily
741 mitigating the outward spread of climate stress. Measures such as controlled grazing
742 and protection of soil seed banks can enhance ecological resilience and provide
743 backup habitats for primary areas (Wang et al., 2021). Tertiary protected areas serve

744 as reserved spaces for future habitats. Although their current conservation value is low,
745 they may become new settlement sites for species under climate change, necessitating
746 low-intensity management to maintain their ecological potential (Farrer et al., 2014b).
747 Together, these considerations establish a three-tiered conservation framework
748 consisting of “primary core areas, secondary buffer zones, and tertiary reserved
749 areas.”

750 From the perspective of climate scenario pathways, the priority conservation
751 areas identified in this study exhibit differentiation under different climate scenarios.
752 Under moderate scenarios (SSP1-2.6 and SSP2-4.5), the reduction in the area of
753 priority conservation zones is relatively small, indicating that conservation efforts
754 should focus on optimizing the existing protected area network. Under high-stress
755 scenarios (SSP3-7.0 and SSP5-8.5), the areas of priority conservation zones further
756 contract toward the southern margin and western parts of the central desert,
757 highlighting the need to proactively identify climate refugia and plan species
758 migration corridors. Future research should advance in three aspects: first,
759 incorporating data on human activities such as grazing and road construction to clarify
760 how anthropogenic disturbances interact with climate stress to affect the effectiveness
761 of protected areas (Geldmann et al., 2019); second, employing field tracking and
762 genomics to determine the actual dispersal range of short-lived plant seeds, providing
763 a basis for corridor design (Cote et al., 2017); third, introducing dynamic process
764 models to upgrade the current static identification of "suitable habitat areas" to a
765 dynamic assessment of "population sustainability," thereby rendering conservation

planning more operational.

The core conclusions of this section can be summarized as follows: an integrated framework that incorporates species diversity hotspots and their potential future loss risks within a unified assessment system; two evolutionary characteristics, namely the contraction of priority conservation areas and their spatial reconfiguration; and a three-level functional zoning, comprising core conservation areas, buffer-support zones, and spatial reservation areas. These results provide direct support for optimizing the conservation network of short-lived plants in the study area.

## 5. Conclusions

This study comprehensively assessed the responses of ephemeral plant diversity to climate change in the Gurbantunggut Desert. The main conclusions are as follows: (1) Currently, species richness of ephemeral plants exhibits a “higher in the south, lower in the north” distribution pattern. By the 2050s, an overall decline is projected, with high-value areas shifting southeastward within the desert, and the magnitude of decline increasing with emission intensity; (2) In the study area, precipitation during the wettest season and precipitation in the driest month are the primary positive drivers of species richness, whereas soil pH shows a significant negative correlation with precipitation in the wettest month. The effects of these factors also display spatial heterogeneity; (3) The climate velocity of precipitation-related variables in the future is generally higher than that of temperature variables, indicating that changes in precipitation patterns constitute the main potential climatic stressor for ephemeral

plant communities; (4) Under future climate scenarios, the areas of priority conservation sites identified in this study are projected to contract significantly, aggregating toward the southern margin of the central desert, the western, and eastern regions under the moderate-emission scenario, and further retreating to two core areas in the southern central and western desert under the high-emission scenario.

The three-dimensional framework of "species diversity hotspot—species loss risk—climate velocity" developed in this study provides a scientific basis for the targeted conservation of ephemeral plants in arid regions and for adaptive management of desert biodiversity under climate change.

## Declarations

### Ethics approval and consent to participate

Not applicable

### Consent for publication

Not applicable

### Availability of data and materials

The datasets used and analysed during the current study are available from the corresponding author on reasonable request.

### Competing interests

The authors declare that they have no competing interests.

## Funding

This work was supported by the National Natural Science Foundation of China (Grant No. 32460094) and the General Project of the Science and Technology Plan of Xinjiang Production and Construction Corps (Grant No. 2025DA069).

## Authors' contributions

XS, XZ, and YX wrote the original draft of the manuscript. All authors reviewed and edited the manuscript. XS performed visualization, validation, and formal analysis. XS and XZ handled the software. XS, XZ and YX contributed to methodology and data curation. SM was responsible for funding acquisition, supervision, and project administration. XH, HS and JZ developed the conceptualization.

## Acknowledgements

We thank the editors and reviewers for their evaluation of this manuscript.

## Reference

1. Watson, J. E., Rao, M., Ai-Li, K., & Yan, X. (2012). Climate change adaptation planning for biodiversity conservation: A review. Advances in Climate Change Research, 3(1), 1-11. https://doi.org/10.3724/SP.J.1248.2012.00001

2. Thomas, C. D., Cameron, A., Green, R. E., Bakkenes, M., Beaumont, L. J., Collingham, Y. C., Erasmus, B. F. N., De Siqueira, M. F., Grainger, A., Hannah, L., Hughes, L., Huntley, B., Van Jaarsveld, A. S., Midgley, G. F., Miles, L., Ortega-Huerta, M. A., Peterson, A. T., Phillips, O. L., & Williams, S. E. (2004). Extinction risk from climate change. Nature, 427(6970), 145–148. https://doi.org/10.1038/nature02121

3. Sheng, D. (2024). Study on the trend of diversity in plant growth forms in the Gurbantünggüt Desert under variable rainfall condition. Shihezi University.

4. Huang, H., Chang, X., Yue, X., & Lv, D. (2016). Responses of NDVI changes to air temperature and precipitation of different sandy landscape areas in the Horqin Sandy Land. Journal of Desert Research, 36(1), 40. https://doi.org/10.7522/j.issn.1000-694X.2015.00087

5. Chen, I. C., Hill, J. K., Ohlemüller, R., Roy, D. B., & Thomas, C. D. (2011). Rapid range shifts of species associated with high levels of climate warming. Science, 333(6045), 1024-1026. https://doi.org/10.1126/science.1206432

6. IPCC, 2022: Climate Change 2022: Mitigation of Climate Change. Contribution of Working Group III to the Sixth Assessment Report of the Intergovernmental Panel on Climate Change [P.R. Shukla, J. Skea, R. Slade, A. Al Khourdajie, R. van Diemen, D. McCollum, M. Pathak, S. Some, P. Vyas, R. Fradera, M. Belkacemi, A. Hasija, G. Lisboa, S. Luz, J. Malley, (eds.)]. Cambridge University Press, Cambridge, UK and New York, NY, USA. https://doi.org/10.1017/9781009157926

7. Bellard, C., Bertelsmeier, C., Leadley, P., Thuiller, W., & Courchamp, F. (2012). Impacts of climate change on the future of biodiversity. Ecology letters, 15(4), 365-377. https://doi.org/10.1111/j.1461-0248.2011.01736.x

8. Zhao, G., Cui, X., Sun, J., Li, T., Wang, Q., Ye, X., & Fan, B. (2021). Analysis of the distribution pattern of Chinese Ziziphus jujuba under climate change based on optimized biomod2 and MaxEnt models. Ecological Indicators, 132, 108256. https://doi.org/10.1016/j.ecolind.2021.108256

9. Fang, Y., Zhang, X., Wei, H., Wang, D., Chen, R., Wang, L., & Gu, W. (2020). Predicting the invasive trend of exotic plants in China based on the ensemble model under climate change: A case for three invasive plants of Asteraceae. The Science of the Total Environment, 756, 143841. https://doi.org/10.1016/j.scitotenv.2020.143841

10. Huang, D., An, Q., Huang, S., Tan, G., Quan, H., Chen, Y., Zhou, J., & Liao, H. (2023). Biomod2 modeling for predicting the potential ecological distribution of three Fritillaria species under climate change. Scientific Reports, 13(1), 18801. https://doi.org/10.1038/s41598-023-45887-6

11. Kanagaraj, R., Araujo, M. B., Barman, R., Davidar, P., De, R., Digal, D. K., Gopi, G. V., Johnsingh, A. J. T., Kakati, K., Kramer-Schadt, S., Lamichhane, B. R., Lyngdoh, S., Madhusudan, M. D., Najar, M. U. I., Parida, J., Pradhan, N. M. B., Puyravaud, J., Raghunath, R., Rahim, P. P. A., . . . Goyal, S. P. (2019). Predicting range shifts of Asian elephants under global change. Diversity and Distributions, 25(5), 822–838. https://doi.org/10.1111/ddi.12898

12. Guisan, A., Tingley, R., Baumgartner, J. B., Naujokaitis-Lewis, I., Sutcliffe, P. R., Tulloch, A. I. T., Regan, T. J., Brotons, L., McDonald-Madden, E., Mantyka-Pringle, C., Martin, T. G., Rhodes, J. R., Maggini, R., Setterfield, S. A., Elith, J., Schwartz, M. W., Wintle, B. A., Broennimann, O., Austin, M., . . . Buckley, Y. M. (2013). Predicting species distributions for conservation decisions. Ecology Letters, 16(12), 1424–1435.

https://doi.org/10.1111/ele.12189

13. Zhu, M., Dong, X., Ling, S., & Luan, B. (2024). Identification of ecological conservation priority areas for key terrestrial wildlife in the Guangdong–Hong Kong–Macao Greater Bay Area. Landscape Architecture Frontiers, 13(6), 58. https://doi.org/10.15302/j-laf-0-020026
14. Lai, Q., Hoffmann, S., Jaeschke, A., & Beierkuhnlein, C. (2022). Emerging spatial prioritization for biodiversity conservation indicated by climate change velocity. Ecological Indicators, 138, 108829. https://doi.org/10.1016/j.ecolind.2022.108829
15. Mao, Z. (1992). Floristic characteristics of early spring ephemeral plants. Arid Zone Research, (01):11-12. https://doi.org/10.13866/j.azr.1992.01.004
16. Mao, Z., & Zhang, D. (1994). The conspectus of ephemeral flora in northern Xinjiang. Arid Zone Research, (03):1-26. https://doi.org/10.13866/j.azr.1994.03.001
17. Li, X., Ma, M., Cui, D., & Cui, N. (1998). Analyses on the characteristics of botanical Species diversity in Xinjiang. Journal of Shihezi University(Natural Science),(04):33-47. https://doi.org/10.13880/j.cnki.65-1174/n.1998.04.004
18. Zhang, L. (2002). Species diversity and ecological distribution of ephemeral plants ( 2 ) in Xinjiang. Life World, (02):4-5.
19. Yuan, S., & Tang, H. (2010). Patterns of ephemeral plant communities and their adaptations to tem-perature and precipitation regimes in Dzungaria Desert, Xinjiang. Biodiversity Science, 18(04):346-354.
20. Zhang, L., & Chen, C. (2002). On the general characteristics of plant diversity of GurbantunggutSandy Desert. Acta Ecologica Sinica, (11):1923-1932. https://doi.org/10.3321/j.issn:1000-0933.2002.11.018

21. Chen, Y., Zhang, L., Shi, X., Liu, H., & Zhang, D. (2019). Life history responses of two ephemeral plant species to increased precipitation and nitrogen in the Gurbantunggut Desert. PeerJ, 7, e6158. https://doi.org/10.7717/peerj.6158

22. Qian, Y., Wu, Z., Zhang, L., Zhao, R., Wang, X., & Li, Y. (2007). Spatial distribution characteristics of ephemeral plants in Gurbantunggut Desert. Chinese Science Bulletin, (19):2299-2306. https://doi.org/10.3321/j.issn:0023-074x.2007.19.015

23. Wang, X., Zhang, Y., Wang, Y., Wan, J., & Xu, M. (2006). Eco-environment change of biological crusts on longitudinal dune surface in Gurbantunggut Desert. Journal of Desert Research, (05):711-716. https://doi.org/10.3321/j.issn:1000-694X.2006.05.007

24. Wang, X., Jiang, J., Lei, J., & Zhao, C. (2004). Relationship between ephemeral plants distribution and soil moisture on longitudinal dune surface in Gurban-tonggut desert. Chinese Journal of Applied Ecology, (04):556-560. https://doi.org/10.13287/j.1001-9332.2004.0120

25. Liu, Z. (2020). Dune landform and its development environment in Gurbantunggut Desert. Shaanxi Normal University. https://doi.org/10.27292/d.cnki.gsxfu.2020.000039

26. Brown, J. L. (2014). SDMtoolbox: a python-based GIS toolkit for landscape genetic, biogeographic and species distribution model analyses. Methods in Ecology and Evolution, 5(7), 694–700. https://doi.org/10.1111/2041-210x.12200

27. Fan, Y., Gao, H., Tao, S., Yin, C., & Yu, X. (2024). Potential distribution prediction of *Pomacea canaliculata* in China based on the Biomod2. Chinese Journal of Applied Ecology, 35(08):2237–46. https://doi.org/10.13287/j.1001-9332.202408.024

28. Ricklin, S., Meyer-Heim, A., & Van Hedel, H. J. A. (2018). Dual-task training of children with neuromotor disorders during robot-assisted gait therapy: prerequisites of patients and

influence on leg muscle activity. Journal of NeuroEngineering and Rehabilitation, 15(1), 82. https://doi.org/10.1186/s12984-018-0426-3

29. Zhang, D., Ma, S., Wei, B., Wang, C., Zhang, L., & Yan, H. (2022). Historical distribution pattern and driving mechanism of Haloxylon in China. Biodiversity Science, 30(01): 42–51. https://doi.org/10.17520/biods.2021192

30. Liu, C., & Guo, S. (2024). Suitability analysis and distribution prediction of *Castanea mollissima* under Climate Change. Scientia Silvae Sinicae, 30. 60(04): 109–18. https://doi.org/10.11707/j.1001-7488.LYKX20220436

31. Thuiller, W., Lavorel, S., Araújo, M. B., Sykes, M. T., & Prentice, I. C. (2005). Climate change threats to plant diversity in Europe. Proceedings of the National Academy of Sciences, 102(23), 8245–8250. https://doi.org/10.1073/pnas.0409902102

32. Chen, Y. (2009). Reconstructing the mathematical process of spatial autocorrelation based on Moran's statistics. Geographical Research, 28(06): 1449–63. https://doi.org/10.11821/yj2009060002

33. Yang, W., Deng, M., Tang, J., & Luo, L. (2022). Geographically weighted regression with the integration of machine learning for spatial prediction. Journal of Geographical Systems, 25(2), 213–236. https://doi.org/10.1007/s10109-022-00387-5

34. Dobrowski, S. Z., & Parks, S. A. (2016). Climate change velocity underestimates climate change exposure in mountainous regions. Nature Communications, 7(1), 12349. https://doi.org/10.1038/ncomms12349

35. Shen, Y., Chen, H., Liu, G., Deng, H., & Su, X. (2024). Conservation gaps and priorities on the Qinghai-Tibetan Plateau based on biodiversity and ecosystem services. Acta Ecologica

933 Sinica, 44(11):4507–16. https://doi.org/10.20103/j.stxb.202310082156
934 36. Işlar, M. (2019). Policy options and tools for decision makers. : IPBES, Global assessment
935 report on biodiversity and ecosystem services of the Intergovernmental Science-Policy
936 Platform on Biodiversity and Ecosystem Services. Lund University Publications (Lund
937 University). https://lup.lub.lu.se/record/76f11db5-720f-48fb-9b3a-9036ef8152f9
938 37. Berdugo, M., Delgado-Baquerizo, M., Soliveres, S., Hernández-Clemente, R., Zhao, Y.,
939 Gaitán, J. J., Gross, N., Saiz, H., Maire, V., Lehmann, A., Rillig, M. C., Solé, R. V., &
940 Maestre, F. T. (2020). Global ecosystem thresholds driven by aridity. Science, 367(6479),
941 787–790. https://doi.org/10.1126/science.aay5958
942 38. Loarie, S. R., Duffy, P. B., Hamilton, H., Asner, G. P., Field, C. B., & Ackerly, D. D. (2009).
943 The velocity of climate change. Nature, 462(7276), 1052–1055.
944 https://doi.org/10.1038/nature08649
945 39. Wang, Y., Liang, E., Lu, X., Camarero, J. J., Babst, F., Shen, M., & Peñuelas, J. (2021).
946 Warming-induced shrubline advance stalled by moisture limitation on the Tibetan Plateau.
947 Ecography, 44(11), 1631–1641. https://doi.org/10.1111/ecog.05845
948 40. Liu, Q., Piao, S., Fu, Y. H., Gao, M., Peñuelas, J., & Janssens, I. A. (2019). Climatic warming
949 increases spatial synchrony in spring vegetation phenology across the northern hemisphere.
950 Geophysical Research Letters, 46(3), 1641–1650. https://doi.org/10.1029/2018gl081370
951 41. Noy-Meir, I. (1973). Desert Ecosystems: environment and producers. Annual Review of
952 Ecology and Systematics, 4(1), 25–51. https://doi.org/10.1146/annurev.es.04.110173.000325
953 42. Van Rooyen, M., Grobbelaar, N., Theron, G., & Van Rooyen, N. (1992). The ephemerals of
954 Namaqualand: effect of germination date on development of three species. Journal of Arid

955 Environments, 22(1), 51–66. https://doi.org/10.1016/s0140-1963(18)30656-6
956 43. Chen, D., Chen, X., Jia, C., Wang, Y., Yang, L., & Hu, X. (2021). Effects of precipitation and
957 microorganisms on persistence of buried seeds: a case study of 11 species from the Loess
958 Plateau of China. Plant and Soil, 467(1–2), 181–195.
959 https://doi.org/10.1007/s11104-021-04990-1
960 44. Li, T., Yang, J., Yao, R., Zhang, L., Xie, W., Wang, X., Tang, C., Li, W., & Yang, J. R. (2025).
961 Effects of Water-Saving management measures on the Water-Salt properties of Saline–Alkali
962 soil and maize yield in Ningxia, China. Agronomy, 15(3), 645.
963 https://doi.org/10.3390/agronomy15030645
964 45. Azevedo, L. B., Van Zelm, R., Hendriks, A. J., Bobbink, R., & Huijbregts, M. A. (2012).
965 Global assessment of the effects of terrestrial acidification on plant species richness.
966 Environmental Pollution, 174, 10–15. https://doi.org/10.1016/j.envpol.2012.11.001
967 46. Yang, F., Xu, J., Zhao, X., Wang, X., & Xiong, Y. (2022). Assessment of the Grassland
968 Ecological Compensation Policy (GECP) in Qinghai, China. Agriculture, 12(9), 1479.
969 https://doi.org/10.3390/agriculture12091479
970 47. Farrer, E. C., Ashton, I. W., Spasojevic, M. J., Fu, S., Gonzalez, D. J. X., & Suding, K. N.
971 (2014b). Indirect effects of global change accumulate to alter plant diversity but not
972 ecosystem function in alpine tundra. Journal of Ecology, 103(2), 351–360.
973 https://doi.org/10.1111/1365-2745.12363
974 48. Geldmann, J., Manica, A., Burgess, N. D., Coad, L., & Balmford, A. (2019). A global-level
975 assessment of the effectiveness of protected areas at resisting anthropogenic pressures.
976 Proceedings of the National Academy of Sciences, 116(46), 23209–23215.

https://doi.org/10.1073/pnas.1908221116

49. Cote, J., Brodin, T., Fogarty, S., & Sih, A. (2017). Non-random dispersal mediates invader impacts on the invertebrate community. Journal of Animal Ecology, 86(6), 1298–1307. https://doi.org/10.1111/1365-2656.12734